UNDERSTANDING THE NEUROPATHOGENESIS OF RIFT VALLEY FEVER USING IN VITRO AND IN VIVO MODELS

by

Michael Robert Kujawa

B.S. Biochemistry, SUNY Geneseo, 2011

Submitted to the Graduate Faculty of

the Department of Infectious Diseases and Microbiology

Graduate School of Public Health in partial fulfillment

of the requirements for the degree of

Master of Science

University of Pittsburgh

2016

UNIVERSITY OF PITTSBURGH

GRADUATE SCHOOL OF PUBLIC HEALTH

This thesis was presented

by

Michael Robert Kujawa

It was defended on

April 12th, 2016

and approved by

Douglas S. Reed, Ph.D.
Associate Professor
Department of Immunology
School of Medicine
University of Pittsburgh

Velpandi Ayyavoo, Ph.D.
Professor and Assistant Chair
Department of Infectious Diseases and Microbiology
Graduate School of Public Health
University of Pittsburgh

Thesis Director: Amy L. Hartman, Ph.D.
Assistant Professor
Department of Infectious Diseases and Microbiology
Graduate School of Public Health
University of Pittsburgh

Amy L. Hartman, Ph.D.

UNDERSTANDING THE NEUROPATHOGENESIS OF RIFT VALLEY FEVER USING IN VITRO AND IN VIVO MODELS

Michael Robert Kujawa, M.S.

University of Pittsburgh, 2016

ABSTRACT

Rift Valley Fever Virus (RFVF) is a mosquito-borne pathogen found primarily within Africa that is capable of causing both human and animal illness. In humans, RVFV can cause different clinical diseases, with encephalitis being one of the more severe outcomes. In order to study the neuropathogenic mechanisms of RVFV, our laboratory developed the Lewis rat model. When exposed to RVFV via the aerosol route, Lewis rats develop a uniformly lethal encephalitic disease with neurological symptoms. The goal of this research study is to compare *in vitro* brain cell culture systems to the *in vivo* brain environment of rats infected with RVFV, further define the systemic (serum) and regional (CNS) cytokine dysregulation that occurs in infected rats, and explore the neuropathogenesis using an animal model. The results presented here demonstrate that SH-SY5Y neuronal cells and HBMEC cells were as permissive for viral replication as Vero E6 and BHK-21 cells, two cell lines that are defective in the antiviral response. The high permissivity of these cells for RVFV replication suggests both cell types may be targeted *in vivo* and play a role in disease progression. Cytokines produced from SH-SY5Y and HBMEC cells *in vitro* are similar to the cytokine storm produced in infected rats during the encephalitic stage of disease. MMP-9 may be a potential factor in compromising brain vasculature, and current studies are continuing to evaluate the effect of virus infection on blood brain barrier integrity.

Experiments examining the blood brain barrier integrity in infected rats suggest that virus arrives in the CNS via the olfactory bulb prior to breakdown of the blood brain barrier. Taken together, the neuropathological route of infection appears to enter through the olfactory epithelium early after exposure and progresses directly into the brain tissue. The public health significance of this project is supported by the creation of a novel Rift Valley Fever in vitro neuronal model, as well as the exploration of the neuropathogenesis during infection that has previously been unknown.

TABLE OF CONTENTS

LIST OF TABLES

LIST OF FIGURES

ACKNOWLEDGEMENTS

1.0   INTRODUCTION

Rift Valley Fever Virus (RVFV) is a member of the *Bunyaviridae* family and the *Phlebovirus* genus. It is a single-stranded RNA enveloped virus composed of both negative and ambisense strands. As with all viruses in the *Bunyaviridae* family, the genome of RVFV is split into three segments; L and M, which are negative sense, and S, the ambisense strand (1). The virus encodes four structural proteins; RNA polymerase (L), glycoprotein Gn (M), glycoprotein Gc (M), and the nucleocapsid protein (S) (1). In addition, RVFV produces three non-structural proteins; NSm1 (M), NSm2 (M), and NSs (S) (1). The NSs protein is the main virus virulence factor.

RVFV is an emerging zoonotic pathogen that affects both humans and domestic livestock primarily in Sub-Sahara Africa, Egypt, and the Saudi Arabian peninsula (2). The virus affects livestock in a greater capacity by causing a 10-20% mortality rate, and a near 100% fatal neonatal abortion storm in pregnant ruminants (2). Fatalities in humans are more limited, with only about 2% of cases progressing to severe complications, and of this only 20% succumbing to disease (3). Although the virus is typically spread through the bite of infected mosquito, evidence has also been presented that the virus can cause disease when inhaled (1).

Of the many severe complications that can develop, one of most worrying ones is encephalitic disease. Data previously generated in our laboratory has shown that at least in animals, RVFV is more likely to cause encephalitis when inhaled in a small particle aerosol (4).

Other viruses in the Bunyavirus family, as well as viruses in the Alphavirus genus, are known to cause encephalitis (5). These neurotropic viruses disrupt the brain to levels that are sometimes beyond repair, destroying the central nervous system along the way (5). The neuropathology followed by these viruses tends to cause fatal encephalitis, entering into the body and progressing to the brain through the blood brain barrier. Understanding the mechanism of neuroinvasion by these pathogens is the first step in combating the serious outcomes that can occur.

1.1   RIFT VALLEY FEVER VIRUS

1.1.1   Epidemiology

RVFV was first recognized as the causative agent of a major disease outbreak in 1930 in the Great Rift Valley of Kenya (1). The virus was discovered after a major rainfall brought about a wave of fatal illness in lambs, as well as a febrile illness in the surrounding human population. Since then, the disease has been found in the far reaches of South Africa, including making the jump over to Madagascar, throughout Eastern Africa reaching up to Egypt, and recently has spread into the Arabian Peninsula in Saudi Arabia and Yemen (1).

Typically, RVFV is spread through the bite of a mosquito, but accidental exposures and experimental data has shown that the virus can also be transmitted via exposure to infected animal tissues and aerosols generated either naturally or mechanically (1), (4). RVFV follows a life cycle typical of the *Phlebovirus* genus and the family (1). This entails a mosquito vector that is necessary for the virus to mature, and uses this victor to spread the disease to the host. The

virus is able to lie dormant in the eggs of these mosquitoes during periods of low rainfall, waiting for the ideal conditions to occur. RVFV has been found in over forty different species of mosquitoes across eight different genera, including the widespread *Aedes* and *Culex* mosquitoes (3).

Rift Valley Fever (RVF) has caused human outbreaks with drastically differing results. The 1977 Egyptian outbreak had at least 18,000 people infected, with some estimates near 200,000, and at least 598 deaths directly attributed to the disease (1). In 1987, 232 people died from an outbreak in the Senegal region, with thousands more infected alongside of mass ruminant abortion storms that set the region's economy back significantly (1). The Saudi Arabian Peninsula experienced a similar outbreak that lasted over four months, ending in over 245 deaths and thousands of lost live stock (1).

1.1.2 Pathogenesis and Host Response

In humans, the disease caused by RVFV typically presents as a self-limited febrile illness (6). The incubation period is typically 4-6 days, in which symptoms then begin occurring with severe chills, dizziness, weakness, headaches, and nausea (6). After the onset of initial symptoms, a fever occurs that can last anywhere from four to ten days (1). In most cases, the symptoms will begin clearing after four days, which is the point in which neutralizing antibodies can be detected clinically against the agent (6). Human infections tend to only go as far as this, but there have been documented cases of much more severe outcomes in 1-2% of those infected (6). The disease from this point splits into three different outcomes if it progresses; vision loss, hemorrhagic fever, or encephalitis.

For those that progress to a state of vision loss, the effects have been documented to occur anywhere from immediately at the start of initial symptoms, to several months later (6). One or both eyes may experience retinopathy, with symptoms that range from a white mass covering the retina, to complete retinal detachment (6). Most patients whom progress to this do not fully recover from the vision loss experienced due to the irreversible destruction caused. However, there are cases of improvement months after infection for those that had a more limited retinal infection (6).

In the most fatal of cases, hemorrhagic fever occurs with very little warning. In addition to the symptoms found early on in the febrile illness, patients may also experience bleeding from the gums and the gastrointestinal mucosal membranes, a reduction in platelet and hemoglobin count, jaundice, and occasionally hepatosplenomegaly (6). It is important to note that direct hemorrhage does not always occur, and in these cases most patients will succumb to liver failure (6). Once these symptoms begin, death occurs within three to six days. Autopsies performed on some of these cases have shown encephalitis caused by the virus, suggesting that the neuroinvasion may play a role in the fatal outcome (6).

Encephalitis is seen when the virus takes a neuroinvasive route into the brain. The direct path that the virus takes during this course of disease is still unclear and is currently being studied in the field. Patients who progress to encephalitis often times do not recover, and may show typical signs of neurological disorders such as seizures (6).

1.1.3   Prevention and Treatment

Currently, there are no FDA approved vaccines or therapeutics against Rift Valley Fever (4). There are a few experimental drugs, but they have limited potential or known side effects that keep them from obtaining proper approval.

The first live-attenuated vaccine was created from the Smithburn strain of RVFV obtained in 1958 (7). This virus was passaged 102 times in mouse brains, and was administered to livestock as a vaccine (1). The vaccine was later refined in 1971 and marketed under the naming of the "modified live virus vaccine" (MLVV), but held a few heavy consequences. Even though it was highly attenuated, the virus used had a high potential for reversion in livestock (7). As such, this worked as a potential candidate, but only within countries where the disease was already endemic (7). This would prove disastrous in a country where Rift has not already spread to naturally as it would effectively be introducing it into the area upon reversion.

The next candidate that surfaced as a formalin-inactivated vaccine named NDBR 103 RVFV (7). Formalin inactivated vaccines are considered safer overall, but are less effective due to repetitive inoculations being required to induce and maintain an immune response (7). The vaccine was administered during Operation Whitecoat, but much of the records including the results are still redacted and unavailable to the public (8). What is known, however, was over 500 people were vaccinated with NDBR 103, with very mild side effects that were non febrile nor life threatening (7). Although released records showed safety and efficacy in the individuals vaccinated, the vaccine was never pushed through for mass production (9).

After the 1977 outbreak in Egypt, the US government began research on another potential vaccine termed MP-12 (7). This was developed by serially passaging two different strains from the outbreak, ZH501 and ZH548, in the presence of 5-flourouracil (10). The resulting live

attenuated mutant that arose from the ZH548 strain was termed MP-12, which contained key mutations in each of the three segments of the genome (10). The MP-12 strain has shown high efficiency in preventing abortions in ewes in late pregnancy with neutralizing antibodies present within the animal (7). However, a low rate of abortion did occur when administered early in pregnancy, along with other adverse side effects in those calves that were born (7). Nevertheless, the US government needed something to protect their military personnel with overseas, and experimentally administered the vaccine to over 100 participants. MP-12 proved to be both safe and effective, although it still requires proper testing through the FDA to obtain a license (7).

Another vaccine being pursued currently is Clone 13, which was isolated from a plaque from an infected patient in Central Africa (7). This vaccine candidate lacks approximately 70% of the NSs open reading frame, effectively eliminating the virulence factor of the virus (7). With the NSs gene missing this much, the chance of the virus reverting is minimal to none, making it extremely safe in theory. Trials in animals thus far have proven effective and safe, and Clone 13 is currently being looked at for veterinary purposes (7).

Since there is no FDA approved therapeutic, the main course of action when a patient develops RVF is to follow palliative care. The likelihood of the disease progressing to serious complications tends to be low, so this level of care is enough in a majority of the cases. Experimental data has shown some success with ribavirin in hamsters and non-human primates, but only reduced the infection and did not completely clear it (11). Flavipiravir (T-705), a broad spectrum antiviral, has also been tested against RVFV. This compound is known to be less toxic, and therefore may prove to be a more suitable agent to combat the virus. Data currently shows that when rats are exposed to aerosols containing the virulent ZH501 strain of RVFV, the

T-705 compound significantly increases both the survival rate of those infected, as well as the life span of those that did succumb to disease (12).

1.2   PUBLIC HEALTH SIGNIFICANCE

1.2.1   Impact on Endemic Regions and the United States

Endemic areas have been hit hard by the Rift Valley Fever, and will continue to be hit until there is a means to stop outbreaks. Outbreaks are sporadic, and while they tend to follow heavy rains, they are still unpredictable since they rely on many factors.

Beyond the loss of human life, the socio-economic impact on affected regions after an outbreak is astronomical. In the Kenya region, the livestock market accounts for nearly 90% of all pastoral income (13). The rainy season tends to coincide with the times when animals are at their healthiest due to an abundance of resources (13). Farm owners who would normally be able to sell their animals for larger profit margins instead find themselves with nothing. In an area where the poverty rate is already 70%, this is often times a death sentence for the longevity of the farm as a business (13). While not all of the animals may die, there is still a lurking fear of infected livestock residing within the herd that drive off buyers. On top of this, not only does a herder lose his or her animals that succumb to infection, but with spontaneous abortion rates near 100%, they also lose their entire next generation of animals (13). With the older generation sick, and the younger generation lost to disease, a farm owner has no other options than to completely start over.

7

Downstream, those that depend on the livestock from these farms also suffer immensely. Butchers, traders, and slaughterhouses all feel the economic wave of loss. Outbreaks cause panic, and panic leads to other nations placing sanctions on the source of a problem. During the outbreaks in Africa and the Arabian Peninsula, countries placed trade bans on all meat from the affected areas to prevent the spread of the virus (13). In addition, restrictions and quarantines were placed on all farms that experienced infection, so even the livestock that survived were unable to be used for trade (13).

All of these measures by outside countries stem from the fear of the virus spreading further across the globe. With its capabilities to be carried by so many different species of mosquitos, the fear is justified. Studies have found that the mosquitos in North America can easily transmit the virus at very high titers (14). Once the virus entered the population, studies further suggest that the white tailed deer could serve as a host for infection, allowing for the permanent establishment of the virus (15). Once brought into the United States, either by accidental or premediated means, Rift Valley Fever would remain in undetectable background levels before it was ever discovered, and by then it would be too late (15). Models suggest that within two years of entering the country, it would reach both boarders and become endemic in every region, and cost over $50 billion to attempt to control the virus (16).

1.2.2 History of Rift Valley Fever and Biological Warfare

One of the greatest concerns with Rift Valley Fever is the potential to be used as a bioweapon. Due to the lack of any licensed vaccines or therapeutics, RVFV presents a potentially devastating danger.

The United States government classifies Rift Valley Fever as a Category A Pathogen by the NIAID, and an overlap Select Agent by the USDA (17). Although several risk assessments have been performed, the overall answer is clear. If Rift were to be intentionally introduced into an area that had previously never seen it, it would become widespread and endemic before it could ever be detected (17). This is facilitated by the fact that there are no rapid tests developed to confirm the presence of the virus in a sample, and all samples need to be conducted under high containment protocols (17).

Although much of the information containing the United States' bioweapon program is still classified, there is still a significant amount of information supporting the use of Rift Valley Fever as a potential weapon. Records indicate that research on RVF started under Eisenhower's administration in the 1950s, and concluded when Nixon ended the biological weapon program in the 1970s (8). At first, RVF was considered an effective tool to use since it could be used as an incapacitating agent. Early strains of the virus in the wild were only known to cause feverish symptoms and a very low mortality rate in humans (18). The virus was mostly going to be used for crippling the economic system of a targeted country through infection of the livestock (18). The government held appeal for a weapon that could cause as much damage as possible to an area without risk of human life loss, and without the use of bombs (8). This virus appeared to fit this description, but there are no records officially indicating that the United States ever loaded it into a device capable of weaponizing it.

During the Egyptian outbreak in 1977, the highly virulent ZH501 strain caused mass destruction everywhere it touched. The mortality rate previously documented at 1%-2% skyrocketed, and the United States happened to have an experimental vaccine when it hit (8). U.S. naval soldiers stationed on the Naval Medical Research Unit No. 3 (NAMRU-3) off the

coast of Egypt were required to receive an injection of the experimental vaccine, with noncompliance ending in termination (19). Although the vaccine resulted in a complete success, it had never been used on humans on record prior (8). There exists some hints at previous vaccines for RFV having been used on subjects during Operation Whitecoat, but almost all of this information remains classified (8).

1.3 ANIMAL MODELS

Table 1. Disease outcome of rodent strains after subcutaneous or aerosol exposure to RVFV.

Rodent Type	Strain	Subcutaneous			Aerosol		
		Average Mortality %	Days to Death	Disease Outcome	Average Mortality %	Days to Death	Disease Outcome
Mouse	BALB/c	100%	2-3 6	Early Hepatic Late Neurological	100%	2-3 6	Early Hepatic Late Neurological
Rat	Wister-Furth	90%	3	Hepatic	100%	4	Hepatic
	ACI	10%	15	Neurological	100%	6	Neurological
	Lewis	0%	N/A	N/A	100%	7	Neurological

Table Data Notes:

Mouse subcutaneous and aerosol data from Smith et al. (2010) (20).

Rat subcutaneous data from Peters and Stone (1982) (21).

Rat aerosol data from Bales et al. (2012) (22).

1.3.1 Mice

The most common mouse used in animal research is the BALB/c strain since they are mass bred for laboratory use. When these mice are subjected to Rift Valley Fever, disease strikes quick, and with lethal results. Within three to six days post infection, over 50% of BALB/c mice develop severe hepatic disease resulting in death (20). Strangely, no virus could be detected in the serum at day two post infection, but by day three viral titers skyrocket (20). Those that survived this, just under half of the total infected, showed signs of successfully clearing the virus from their liver and blood, only to succumb to encephalitic disease between days six and nine (20). Viral testing by plaque assay showed virus tropism outwards from the liver beginning as early as day three, showing that the spread was just too fast for the mice to clear before it entered the brain (20). Interestingly, the same results occurred regardless of the route of infection, whether it was subcutaneous or aerosol (20).

Mice provide a good early animal model when initially testing viral pathogenesis or experimental therapeutics. However, due to the speed and lethal efficiency with which Rift Valley Fever is able to infect these mice, they are not the best candidates to replicate human disease. While they show the same symptoms in severe cases, the onset is too rapid with little warning, which is not useful in a therapeutic situation due to the lack of disease markers.

1.3.2   Rats

Just like mice, rodents are also an ideal choice for an animal model due to their relatively low cost and comparability to human biological systems. In the case of Rift Valley Fever, the strain of rat and route of exposure dramatically determines the disease course and outcome of the animal after infection.

For example, Wistar-Furth rats experience a mortality rate of ~90% when infected subcutaneously. ACI rats have only approximately a 10% mortality rate by sub-cutaneous infection, and live about five times longer than Wister-Furth rats under these conditions (22). Lewis rats, however, appear to be almost completely resistant to sub-cutaneous infection with RVFV, but all three of these rats have a 100% mortality rate when subjected to aerosol exposure (22).

Not only are the mortality rates different, but the clinical disease associated is also affected by the breed and exposure route. Previous studies from our lab have provided a model for infection via aerosol on Lewis rats that replicates the encephalitic form of the disease with a 100% reproducibility rate (23). Since this is the route of exposure that the Department of Defense is most concerned with, as well as the outcome they are most concerned about, this model perfectly fits the criteria for the studies performed in this thesis and the future work of the Hartman laboratory.

1.3.3 Nonhuman Primates

In general, infection of non-human primates has provided results with wildly different results. Just like rats, the route of infection and the specific species play a vital role in determining the outcome of the disease.

Nonhuman primates were first documented in research use in 1931, when rhesus macaques were infected and monitored for disease (24). The animals developed a febrile illness, but did not succumb to disease despite producing viremia (24). Although they were infected via intraperitoneal, intracerebral, intranasal, and subcutaneously, the inoculum was derived from the tissues and blood of other infected animals (24). Studies moving forward from this used strains known to be virulent in humans.

When rhesus macaques are infected intravenously with the virulent ZH501 strain, studies have shown a mortality rate around 18%, with around 59% of the infected total displaying clinical illness similar to human infection (24). However, using this setup presents two major flaws. First, intravenous is not the typical route of exposure, since mosquitoes infect extraneously. On top of this, a model with only a 18% mortality rate is ineffective for therapeutic testing (24). An ideal model would be both lethal and mimic human clinical disease.

Since exposure to Rift Valley Fever by aerosol has been documented in both humans and animals, recent studies have turned to aerosolizing the virus. When African Green Monkeys and common marmosets were exposed to the virus, they succumbed to disease despite showing high antibody counts against it (4). The animals all showed signs of neurological disease indicative of encephalitis, providing the groundwork for an animal model for encephalitic disease (4).

1.4 NEUROPATHOGENESIS OF ENCEPHALITIC VIRUSES

1.4.1 Rift Valley Fever

At this time, not much is known regarding the neuropathogenesis of Rift Valley Fever. All of the major outbreaks have seen cases of encephalitis caused by RVFV, but the percentage of cases between outbreaks varies wildly from 10% to nearly 89% within severely hospitalized patients (5). Histological examinations of the brain have shown a mass breakdown of cerebral neurons, as well as focal areas of necrosis where there was an influx of macrophages and lymphocytes (5). However, the exact sites of cerebral infection, as well as the specific types of cells within the brain that are targeted by RVFV, are not yet understood.

Until recently, there was not a good model for encephalitic RVF, which has hindered studies into the neuropathogenesis of this disease. Our lab has developed an animal model that can result in encephalitic disease reproducibly in Lewis rats when exposed to a small particle aerosol containing RVFV (22). Research now is aimed at addressing the route of infection and the role of the blood brain barrier as a possible route of pathogenesis.

1.4.2 Other Encephalitic Viruses

Other encephalitic viruses have been studied and understood much more thoroughly. The principles of their neuropathogenesis may not be exactly the same, but do provide starting points for the lesser known encephalitic viruses such as those in the Bunyavirus family.

Viruses in the *Flaviviridae* family are particularly well studied in their route of infection. Japanese Encephalitis Virus (JEV), a member of this family, is an arthropod-borne virus that is

responsible for large outbreaks in the across Asia (5). As with Rift Valley Fever, JEV causes a febrile illness that can last for a week to two weeks, causing major clinical disease in 1% of infected individuals (5). However, within this group of infected, fatal encephalitis occurs at a rate of nearly 20% (5). Seizures and focal neurological deficits are common clinical manifestations (5). During infection, the virus induces a storm of cytokines and chemokines within the host. Among these, and of particular interest in the research for RVF, is the inducement of MMP-9 (25). MMP-9 is a known factor in the opening of the blood brain barrier, invasion of neuronal tissue by immune cells derived from the blood, and cellular damage or death (25). During JEV infections, MMP-9 is upregulated to levels that allow the virus to cross the blood brain barrier and enter the brain (25). A signaling cascade induced by the JNK1/2 and multiple MAPK pathways leads to NF-κB activation, ultimately leading to the MMP-9 increase (25). From here, the virus is free to infect the brain with devastating results. The entire brain will appear swollen due to lymphocytic infiltration of the grey matter throughout the brain (5).

Alphaviruses, though not as well known in their encephalitic disease course, have been researched heavily to determine their route of pathogenesis. An example from this pool is Venezuelan equine encephalitis virus (VEEV), highly regarded as one of the most important encephalitic alphaviruses due to its history in humans. Although less than 1% of infected individuals will develop encephalitis, outbreaks of the virus tend to involve tens of thousands of human cases, making this small percentage a number to be respected (5). VEEV targets the spleen, lymph nodes, liver, lungs, and CNS, making it diverse and difficult for the body to overcome infection (5). Moderate congestion and edema with hemorrhage can be found in some of these organs, but most importantly in the brain in fatal encephalitic cases (5). Recent research has suggested that, among others, primary sites of infection may stem from B cells and cortical

neurons, supporting the presence of lesions that occur on the brain (5). The exact entry of the virus into the brain is currently being studied.

2.0   STATEMENT OF PROJECT AND SPECIFIC AIMS

In studying an encephalitic disease that affects humans, models must be set up to experimentally simulate the disease in a manner that recapitulates the human disease as much as possible. This can be accomplished with both *in vitro* cell culture models, as well as established animal models. The overall goal of this research study will compare *in vitro* cell culture systems to the *in vivo* brain environment of rats infected with RVFV. Our hypothesis is that RVFV infection of SH-SY5Y cells (human neuronal cell line) and human brain vascular endothelial cells (which represent the blood brain barrier) will induce a comparable cytokine/chemokine response as seen in the brain of infected rats and will therefore be suitable in *in vitro* cell culture models for further study for the neuropathogenesis of this emerging infectious disease. Studying the effect of RVF on brain cells both *in vitro* and *in vivo* will contribute to the overall understanding of the neuropathogenesis of RVFV.

2.1   AIM 1: ASSESS THE SUSCEPTIBILITY OF HUMAN NEURONAL AND BRAIN VASCULAR ENDOTHELIAL CELLS TO INFECTION WITH RVFV

Permissivity of the neuronal cell line SH-SY5Y to RVFV infection will be compared to Vero E6 and BHK-21 cells.

- Viral growth curves will be performed in all 3 cell lines at two different MOIs to compare.

- Viral growth will be measured by plaque assay.

- Viral growth in SH-SY5Y cells will be assessed using GFP-tagged RVFV and fluorescence microscopy.

Permissivity of human brain vascular endothelial cells to RVFV infection will be evaluated.

- Two brain vascular endothelial cell lines will be evaluated (HBMECs) for susceptibility to RVFV infection.

- Infection of each cell line will be compared in 2D and 3D configurations. Viral titers will be measured by plaque assay.

- Parallel infections with RVFV-GFP will be conducted and susceptibility will be evaluated by fluorescence microscopy

2.2 AIM 2: COMPARE CYTOKINE/CHEMOKINE PRODUCTION FROM *IN VITRO* CELL LINE MODELS TO *IN VIVO* RAT INFECTIONS

Preliminary data from rat brain samples have shown increased expression of MCP-1, M-CSF, and Gro/KC at end-stage disease.

- Test supernatants from SH-SY5Y and HBMEC cells for the presence of MCP-1, M-CSF, and Gro-α, IFN-λ, IL-8, RANTES, and IFN α/β by ELISA.

- Rat brain samples have not been tested for MMP-9 and IFN- α/β, yet these proteins may have significant effects on viral pathology.

2.3   AIM 3: IDENTIFICATION OF THE PATHWAY OF NEUROTROPIC DISEASE IN LEWIS RATS

Assessment of the progression of encephalitic disease in Lewis rats after aerosol exposure.

- Injection of fluorescein salt to monitor for breakdown of blood brain barrier.

- Quantification of viral titers in the brain following infection via aerosol.

  o Comparison to other tissues (cervical lymph nodes, lungs, etc.)

- Use of imaging agents during RVFV infection.

  o Allows for live imaging to watch the progression of virus without a need for euthanization

3.0   MATERIALS AND METHODS

3.1   BIOSAFETY

All experiments using the live virulent ZH501 strain of Rift Valley Fever were performed in the Regional Biocontainment Laboratory at the University of Pittsburgh. This facility is approved by DSAT and the USDA to work with Tier 1 Select Agents. All work was conducted in a class II biosafety cabinet connected to an external HEPA filter where no air was recirculated into the lab. Every worker was required to abide by Biosafety Level 3 practices, and used a powered air purifying respirator (3M Versaflo TR-300 PAPR unit) within the containment labs. All animal work was performed under Animal Biosafety Level 3 practices, and operated under strict IACUC approval. For decontamination, Vesphene IIse in a 1:128 dilution was used with a minimum contact time of fifteen minutes before being marked for further decontamination via autoclave.

3.2   CELL CULTURE

Vero E6 (ATCC CRL-1586) and BHK-21 (ATCC CCL-10) cells were passaged and maintained under normal maintenance procedures. Twice a week, the cells were washed with D-PBS (without calcium or magnesium), and then 0.05% EDTA trypsin was added to detach the

monolayer from the flask. Once the cells were detached, D10 media (500mL 1x DMEM from Corning Cellgro, 50mL heat inactivated FBS, 5mL L-Glutamine, and 5mL Pen/Strep) was added to deactivate the trypsin, and the cells were added to a fresh flask at a 1:10 dilution with fresh D10 media. The SH-SY5Y (ATCC CRL-2266) cells were passaged differently than suggested by the ATCC. Once a week, the cells were washed twice with PBS, and then a third amount of PBS was added to the flask. The flask was then gently tapped while swirling the PBS, detaching the monolayer from the flask. The cells were then spun in a centrifuge at 1,200 rpm for seven minutes. The cells were then reconstituted in D10 media, and passed at a dilution of 1:2 with fresh D10 media.

3.3   VIRAL INFECTION AND PROPAGATION

For each infection, the cellular monolayers were grown to a confluency of 85%-90% in a T75 flask. At this point, either RVFV ZH501 or GFP-tagged RVFV was added at an MOI of 0.1 or 1.0 in a total volume of two mL. The viral overlay sat on the monolayer in an incubator with occasional rocking for one hour, before it was removed and fresh D2 growth media was added. The length of each infection varied based on the desired time points, but significant CPE at the 72 hour mark post infection prevented any time points past this. Imaging was performed on a microscope with a digital camera attached, using Spot Basic software. A subsequent experiment using a GFP-tagged RVFV used live cell imaging to monitor the progression of infection, which was performed with the assistance of Timothy Sturgeon.

3.4 PLAQUE ASSAY

To determine viral titers via plaque assay, Vero E6 cells were seeded in a six well plate with D10 media at a high density one day before to ensure confluency around 90% on the day of the experiment. The virus to be titered was then serially diluted in D2 media at a 1:10 dilution, typically out to 10^{-6}. For each dilution, 200 µL were added to each well in duplicate, and then incubated for one hour with occasional rocking. After an hour, the virus was removed, and replaced with 3 mL of a 1:1 mixture of nutrients and agar. Once the mixture solidified and created a gel, these were placed back in the incubator for three days. After three days, two mL of 37% formaldehyde was added to each well for a minimum of three hours to fix them. The formaldehyde, as well as the gels after fixation, were disposed of as chemical waste. The cells were then washed with distilled water and stained with crystal violet. The resulting plaques were then counted from each duplicate, averaged, and used to determine the viral titer.

3.5 TCID50 ASSAY

To determine viral titers via TCID50, a 96 well plate with 4 replicates was used. First, 100 µL of virus was added to 900 µL of D2 media to create a 1:10 dilution. Then, 100 µL of D2 media was added to every well on the plate except wells A1 – D1, the first four wells. In these first four, 150 µL of the virus dilution was added to each well. Next, 50 µL was titered throughout the plate working from A1 – D1 down to A12 – D12. At this point, the titration continued down on the second row from E1 – H1 down to E11 – H11. Wells E12 – H12 were all left untitered to serve as a negative control. Finally, 100 µL of freshly passed Vero E6 cells at a

dilution of 1.5 x 10^5 in D2 media were added to every well. After 4-5 days, viral titers were calculated by visual scoring and use of Reed-Muench calculations.

3.6   GFP IMAGING OF FIXED PLATES

Six twelve well plates were set up containing SH-SY5Y cells in six wells each and infected with the GFP-tagged RVFV. Of these six wells, three were infected at 0.1 MOI and three were infected at 1.0 MOI to effectively produce each sample in triplicate. Each plate was given a time point from 12 hours post infection to 72 hours post infection at 12 hour intervals. At the designated interval, the supernatant was pulled off and frozen, and the plates were fixed in 4% PFA for 24 hours to ensure decontamination. The plates were then taken out of the RBL and into a BSL-2 lab for fluorescent imaging.

3.7   AEROSOL

An aerosol exposure was performed by Dr. Douglas Reed and his lab to infect Lewis rats to the virulent ZH501 strain of RVFV. Each of the rats in these experiments inhaled 3 x 10^4 pfu of ZH501. Following the aerosol, rats were randomly selected in groups of three and serially sacrificed for seven days following exposure. After euthanization, the various tissues, including the brain tissue, from each of these rats were extracted from the skull, homogenized, and stored at -80°C for further testing.

3.8   CYTOKINE AND CHEMOKINE TESTING

MCP-1, M-CSF, Gro-alpha, IL-29, IL-8, RANTES, MMP-9, and IFN-a/b were tested with a custom multiplex panel (Procarta) that had markers for these analytes. The samples that were tested consisted of SH-SY5Y cells at various time points during infection, as well as rat brain samples from serial sacrifices. Multiplex plates were run on a Luminex machine with the help of Timothy Sturgeon inside of the RBL.

3.9   2D AND 3D HBMEC MODELS

HBMEC cells were obtained from Dr. Carolyn Coyne. These blood brain barrier epithelial cells were grown both in a monolayer in a 2D format, and on latex beads in a special incubator set up that allows the cells to grow in a spherical model around the bead for a 3D format. These were then infected with both wild type RVFV and GFP RVFV to assess how the virus affected blood brain barrier cells in vitro in a model that suggests similar pathology to in vivo. Plaque assays were performed to assess for viral titer.

3.10   IVIS IMAGING

All imaging took place within the RBL rodent suite under ABSL-3 conditions. The rats were anesthetized with ketamine/xylazine, and then injected via tail vein with the reagent being used at the time (Reagents used; FITC Salt [Sigma Aldrich], Superhance 680 [Perkin Elmer]). Each reagent was allowed to circulate within the rat for the amount of time suggested by the manufacturer, after which each rat was lightly anesthetized under isoflourene for imaging. Using the excitation and emissions that complemented each reagent, the rat's heads or whole bodies were imaged to assess for the presence of the reagent. A Spectrum CT In Vivo Imaging System (IVIS; Perkin Elmer) was used to image rats. In cases assessing for blood brain barrier permeability, the rat's brains were extracted for *ex vivo* imaging as well. These images were then analyzed to create a logarithmic gradient to better show the areas that were infiltrated by virus / reagent. This gradient was color coded with a scale included to visually show changes between the infected and uninfected animals.

3.11   PCR

Infectious materials that were to be analyzed by PCR were first inactivated using a protocol that was approved by the University of Pittsburgh RBL Biosafety Officer. To do this, 100μL of serum or homogenized tissue sample was added to 900μL of Trizol reagent in an Eppendorf tube, capped and inverted vigorously for thirty seconds, and then allowed at least five minutes contact time for full inactivation. The samples were then transferred to a new Eppendorf tube, where they were stored until ready for RNA extraction.

RNA extraction was performed using the spin column method with the use of Ambion RNA extraction kits. The final samples were run in duplicate in a 96 well plate against known standards, and quantified based on the standard curve generated from each plate. PCR results were reported in relative pfu/mL based on prior calculations generated by comparing standards to plaque assay results.

4.0   RESULTS

4.1   AIM 1: ASSESS THE SUSCEPTIBILITY OF HUMAN NEURONAL AND BRAIN VASCULAR ENDOTHELIAL CELLS TO INFECTION WITH RVFV

To assess the susceptibility of a human neuronal cell line, SH-SY5Y (ATCC CRL-2266) cells were grown in previously described D10 media and observed for natural characteristics (Figure 1). SH-SY5Y cells were cultured by JL Biedler in 1970, and given to the ATCC from a four year old human female with neuroblastoma, after which the cells were immortalized. In our hands, the cells grew very slowly during days one to four post maintenance, and then grew quicker during days five to seven. By day seven, they were considered to be confluent enough to passage. SH-SY5Y cells grew in long spindle like fashion with small filaments coming off the ends. If left past confluency, these cells typically clumped up and came off of the monolayer in large cellular rafts.

Day 5	Day 6	Day 7
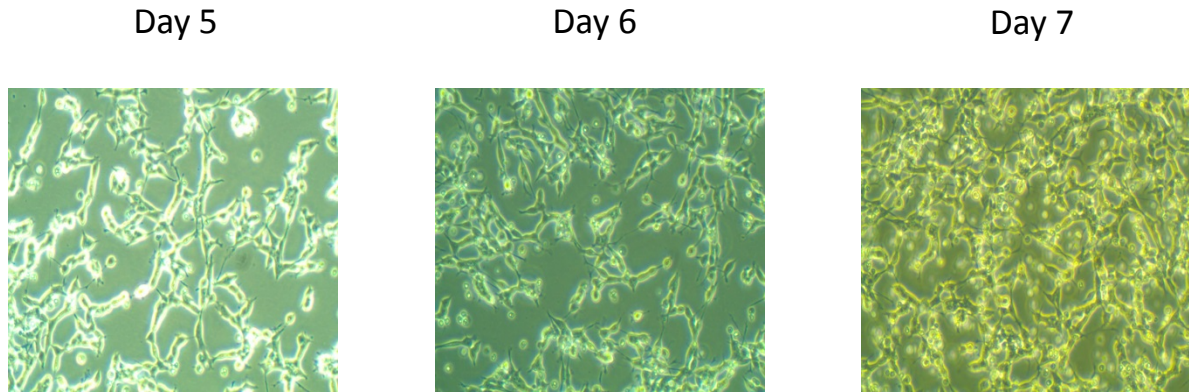
Figure 1. Uninfected SH-SY5Y Cells

SH-SY5Y cells were grown in the presence of D10 media and typically passaged every seven to eight days. Pictures were taken at various time points as they approached confluency. All images were taken at 10x magnification.

When SH-SY5Y cells are infected with RVFV, they appeared like their uninfected over-confluent counterparts in that they slowly began to congregate together, before coming off the monolayer in large masses. Cells infected at a MOI of 0.1 (Figure 2) exhibited these characteristics about twelve hours slower than cells infected at a MOI of 1.0 (Figure 3).

0.1 MOI 12hpi

0.1 MOI 48hpi

0.1 MOI 24hpi

0.1 MOI 60hpi

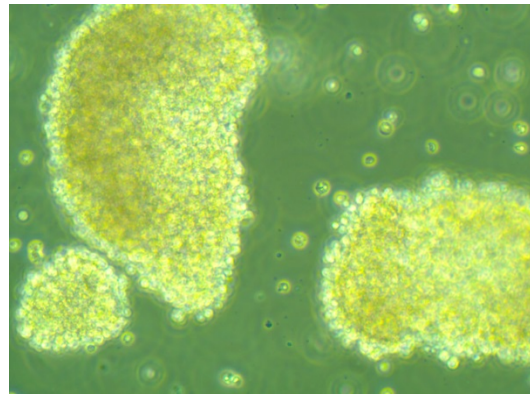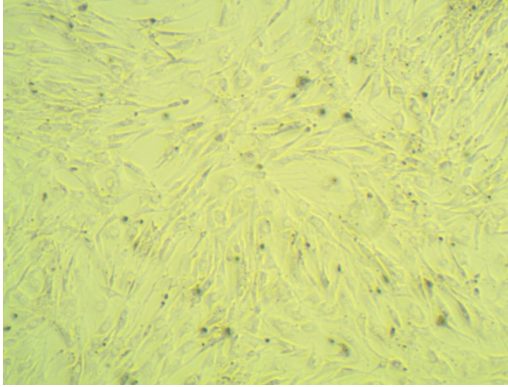## 0.1 MOI 36hpi

0.1 MOI 72hpi
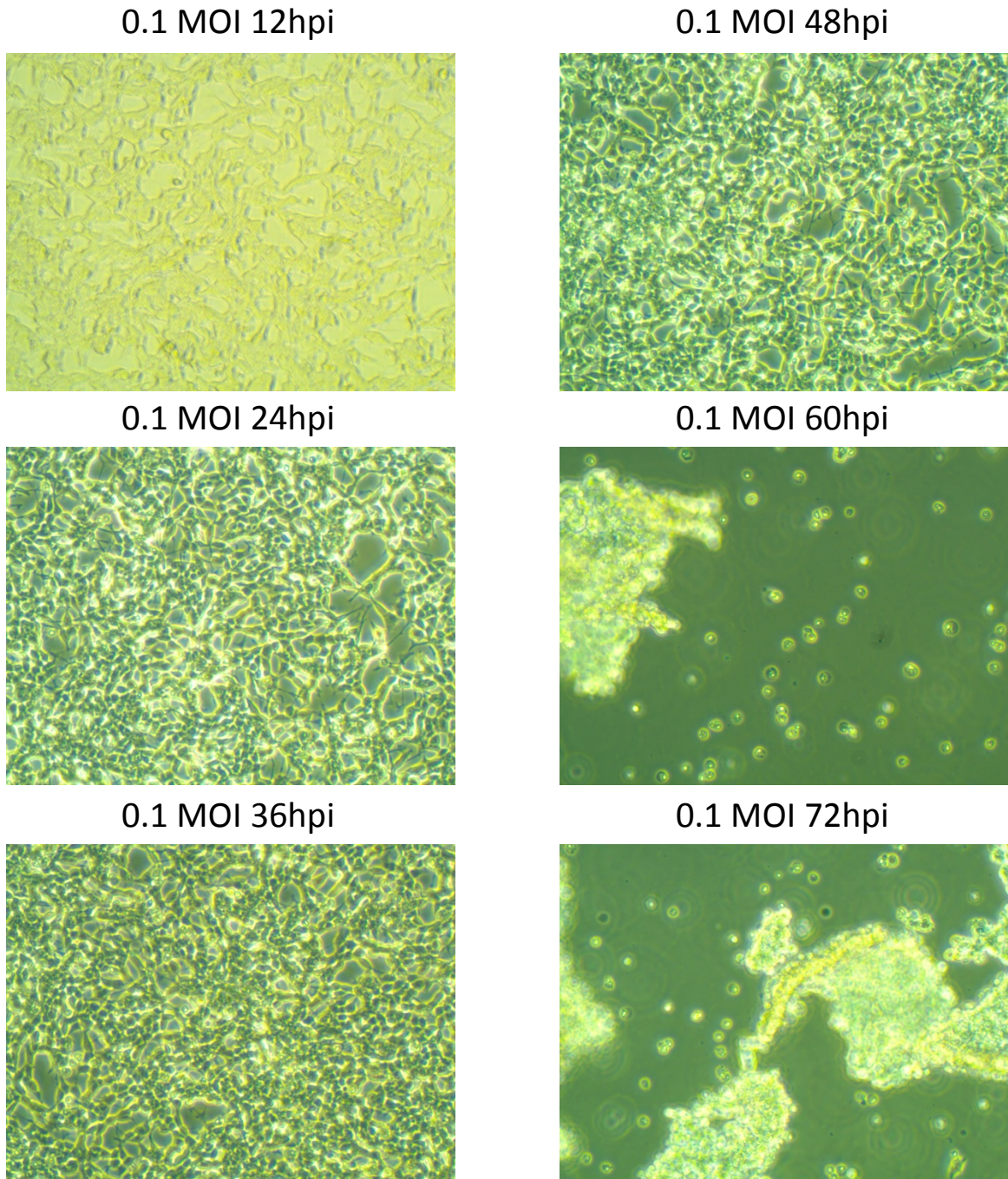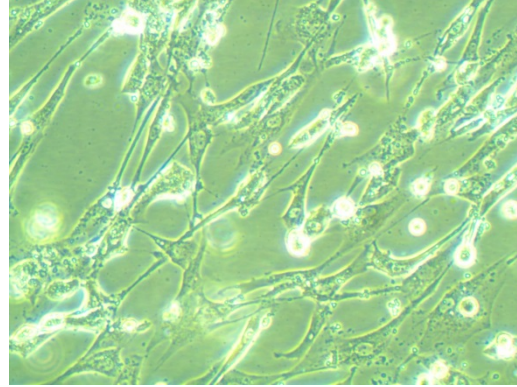
Figure 2. SH-SY5Y Cells Infected at 0.1 MOI

SH-SY5Y cells were infected with RVFV ZH501 at 0.1 MOI, and imaged every twelve hours starting at 12 hours post infection and ending at 72 hours post infection. All images were taken at 10x magnification. Images show a progression in cytopathic effect over time.

1.0 MOI 12hpi
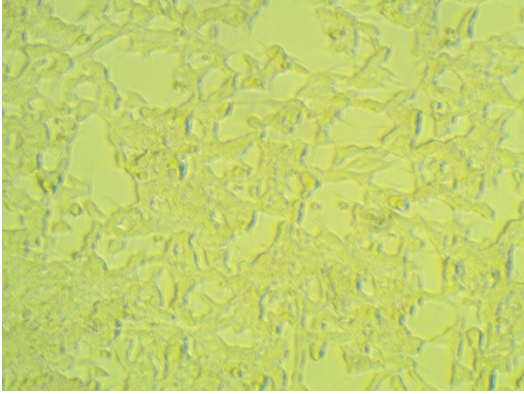
1.0 MOI 48hpi
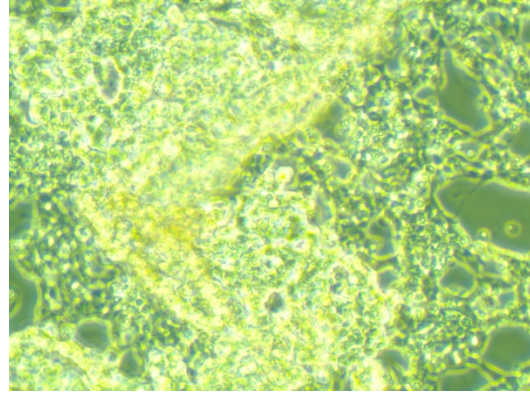
1.0 MOI 24hpi
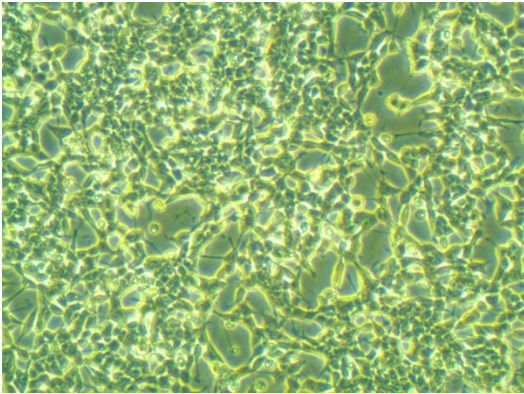
1.0 MOI 60hpi
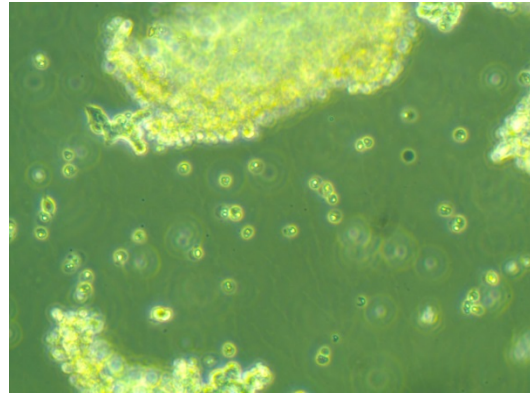
1.0 MOI 36hpi
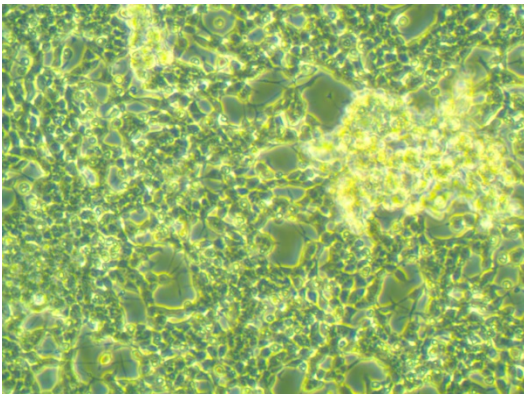
1.0 MOI 72hpi

Figure 3. SH-SY5Y Cells Infected at 1.0 MOI

SH-SY5Y cells were infected with RVFV ZH501 at 1.0 MOI, and imaged every twelve hours starting at 12 hours post infection and ending at 72 hours post infection. All images were taken at 10x magnification. Images show a progression in cytopathic effect over time.

Morphological changes of infected BHK-21 and Vero E6 cells, two commonly used cell lines for RVFV propagation, were compared to SH-SY5Y cells. These cell lines are commonly used in laboratory work for viral infection and propagation due to their deficiency in certain aspects of the antiviral response. BHK-21 cells grew in very long striated patterns that resemble long grains of rice. When they are infected, they will form small clumps and round up either in the middle of the cell, or the whole cell itself will do so. Cells infected at 0.1 (Figure 4) and 1.0 MOI (Figure 5) show the same characteristics, with early viral infection at 48 hours post infection apparent in the cell rounding. Vero E6 cells, on the other hand, grow in a cobblestone fashion. Infected cells at both 0.1 (Figure 6) and 1.0 MOI (Figure 7) both show significant rounding and come off the flask after 36 hours post infection.
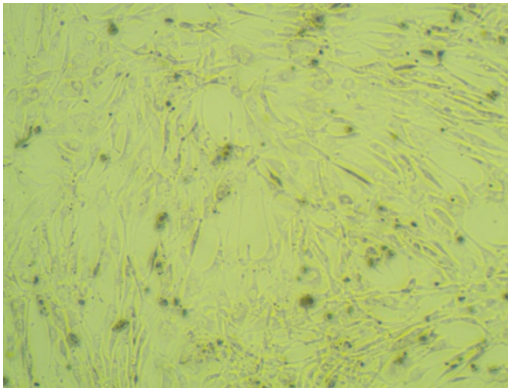
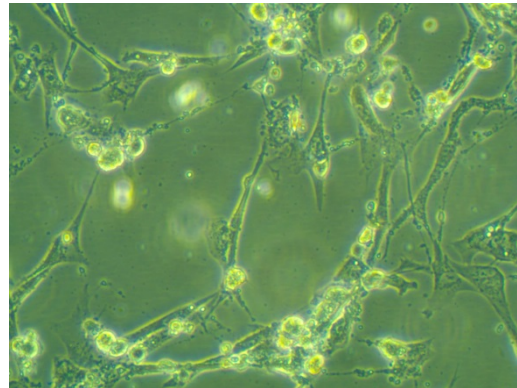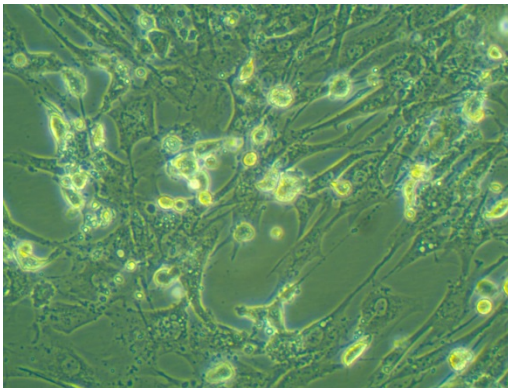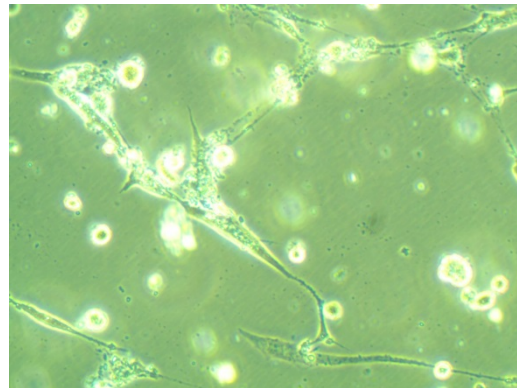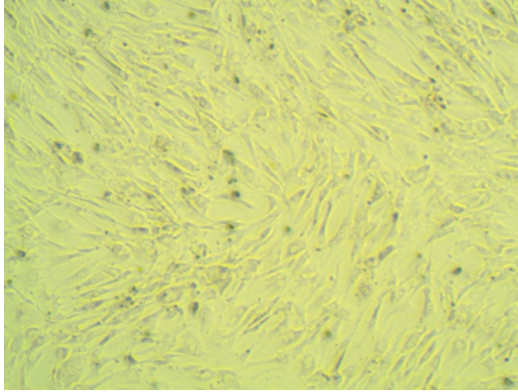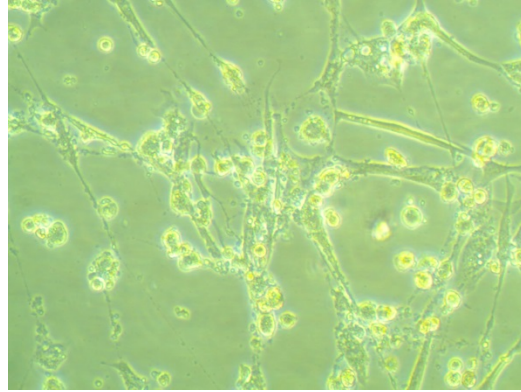**Figure 4. BHK-21 Cells Infected at 0.1 MOI**

BHK-21 cells were infected with RVFV ZH501 at 0.1 MOI, and imaged every twelve hours starting at 12 hours post infection and ending at 72 hours post infection. 12hpi and 24hpi images were taken at 10x magnification, all others were taken at 20x magnification. Images show a progression in cytopathic effect over time.

1.0 MOI 12hpi

1.0 MOI 48hpi

1.0 MOI 24hpi

1.0 MOI 60hpi

1.0 MOI 36hpi

1.0 MOI 72hpi

Figure 5. BHK-21 Cells Infected at 1.0 MOI

BHK-21 cells were infected with RVFV ZH501 at 1.0 MOI, and imaged every twelve hours starting at 12 hours post infection and ending at 72 hours post infection. 12hpi and 24hpi images were taken at 10x magnification, all others were taken at 20x magnification. Images show a progression in cytopathic effect over time.
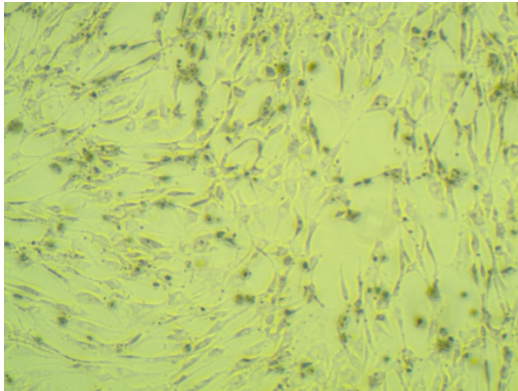
34
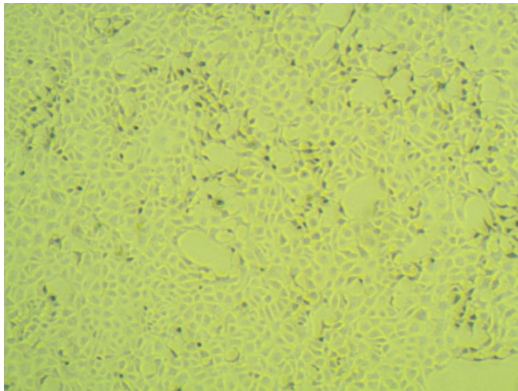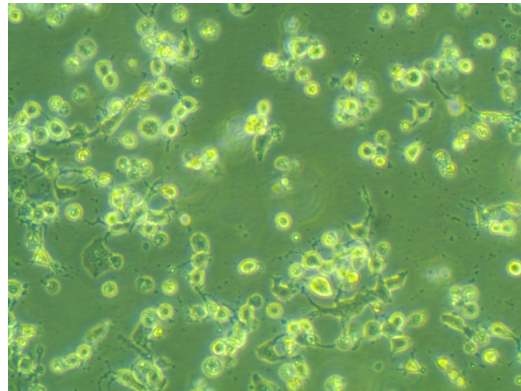
Figure 6. Vero E6 Cells Infected at 0.1 MOI

Vero E6 cells were infected with RVFV ZH501 at 0.1 MOI, and imaged every twelve hours starting at 12 hours post infection and ending at 72 hours post infection. 12hpi and 24hpi images were taken at 10x magnification, all others were taken at 20x magnification. Images show a progression in cytopathic effect over time.
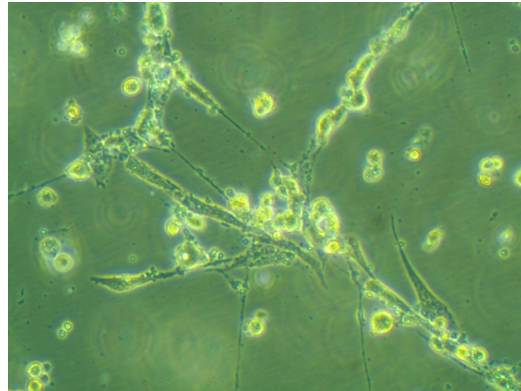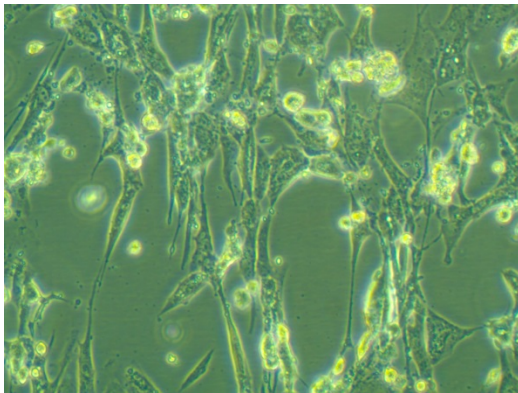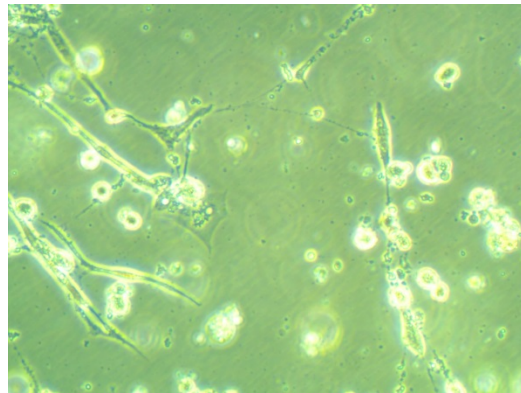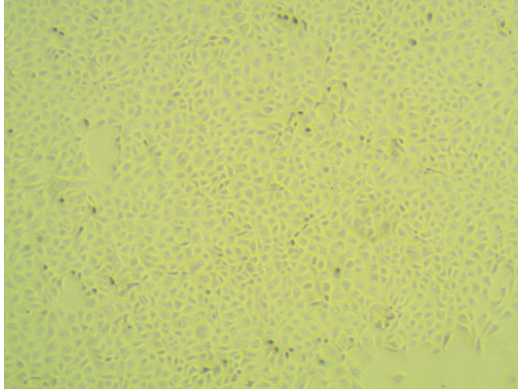
1.0 MOI 12hpi

1.0 MOI 48hpi

1.0 MOI 24hpi

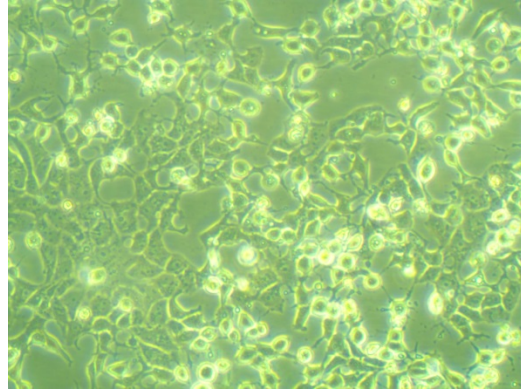**1.0 MOI 60hpi**

1.0 MOI 36hpi

1.0 MOI 72hpi

Figure 7. Vero E6 Cells Infected at 1.0 MOI

Vero E6 cells were infected with RVFV ZH501 at 1.0 MOI, and imaged every twelve hours starting at 12 hours post infection and ending at 72 hours post infection. 12hpi and 24hpi images were taken at 10x magnification, all others were taken at 20x magnification. Images show a progression in cytopathic effect over time.

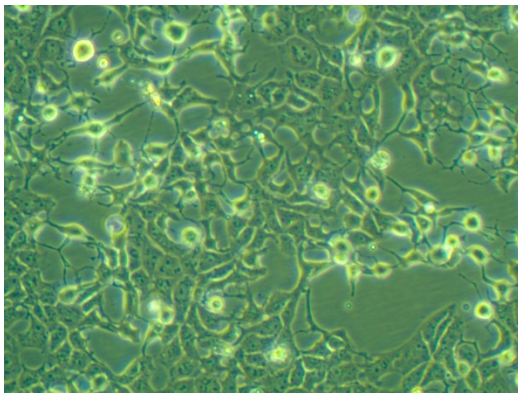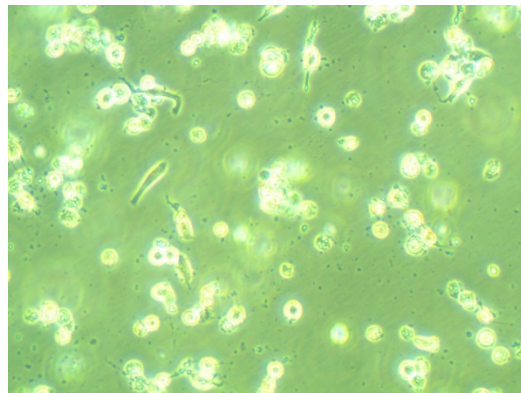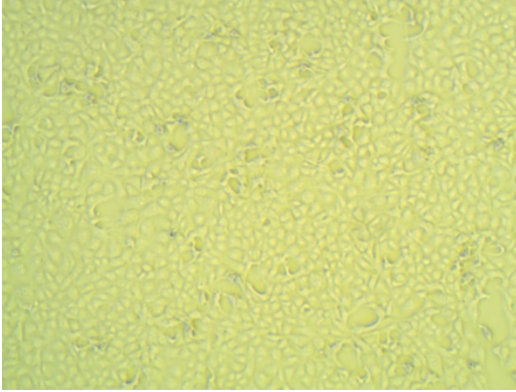Next, the viral titers were determined in each of the three cell lines during infection to assess the permissivity of them to Rift Valley Fever. Supernatant samples were harvested every twelve hours from BHK-21, Vero E6, and SH-SY5Y cells infected at 0.1 and 1.0 MOI. The supernatants were then tested by plaque assay and graphed on a logarithmic scale (Figure 8). For most of the cell lines, viral growth increased the greatest around the 36 and 48 hour post infection time points, and then continued upwards at a slightly slower pace afterwards. In all cases, the 1.0 MOI infected cells had a higher viral titer than their 0.1 MOI counterparts.
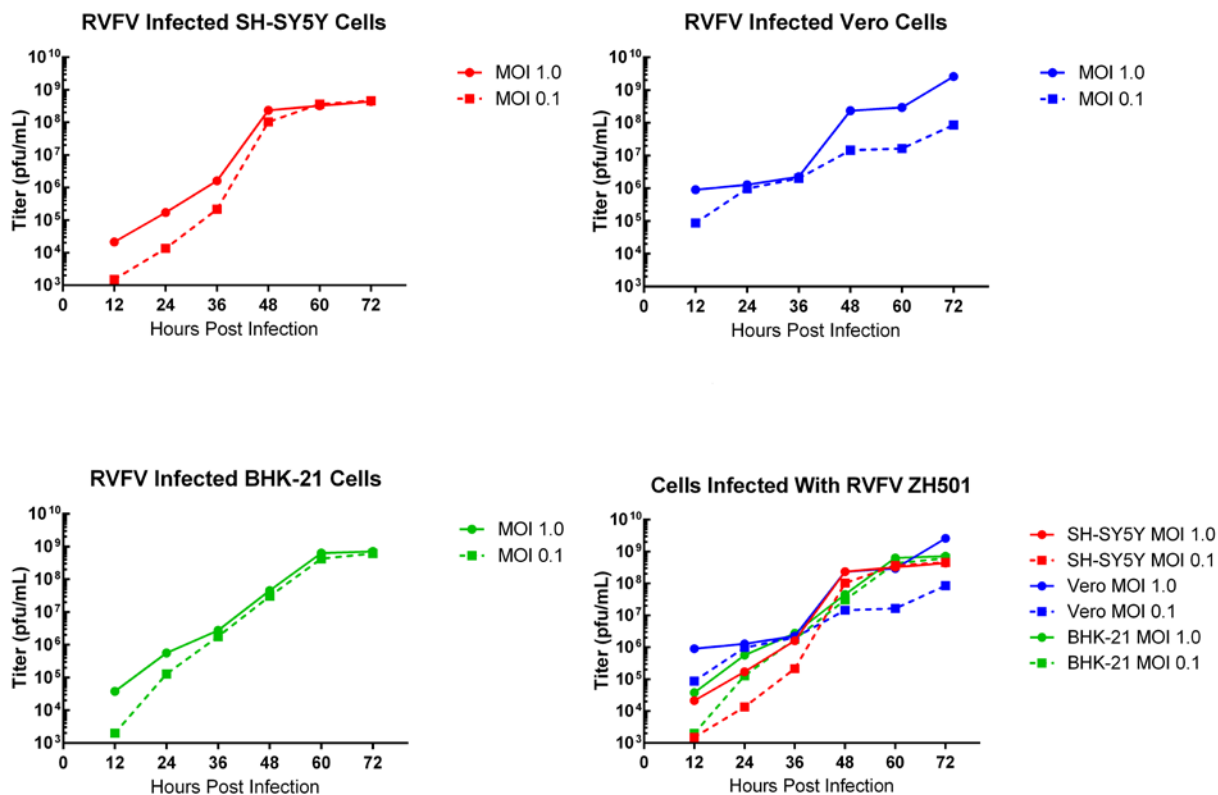
Figure 8. Viral Growth Curves

Viral titer of RVFV ZH501 was assessed for each cell line and multiplicity of infection and graphed for comparison.

Titers were performed by plaque assay, and compared on a logarithmic scale.

A recombinant RVFV expressing the green fluorescence protein (GFP) in place of the NSs protein on the S segment of the genome allows for the observance of the virus throughout the time course of infection. Under live cell imaging on unfixed cells, the virus was seen within the monolayer of SH-SY5Y cells at 48 hours post infection, and in even greater abundance at 72 hours post infection (Figure 9). Due to time restrictions using the live cell imaging machine within the RBL, the infection could only be observed at these time points.

Figure 9. SH-SY5Y Cells Infected with RVFV-GFP

SH-SY5Y cells were infected with GFP-tagged RVFV and live imaged at 48 and 72 hours post infection. GFP foci represent viral areas of cellular syncytia, as well as clumps of cells that have detached from the monolayer.

To take a closer look at the progression of infection every twelve hours post infection, the cells needed to be fixed. To view the infected cells under BSL-2 conditions outside of the RBL, SH-SY5Y cells were infected in plates with the GFP-tagged RVFV and fixed with 4% PFA for twenty four hours at various time points. After fixation, the plates were removed from the RBL and visualized under a fluorescent microscope located in the BSL-2 lab. At 24 hours post infection, a few spots could be seen lighting up within the cells, before morphological changes could be observed (Figure 10). The bright light microscopy pictures were initially taken with a green filter for this first time point. All subsequent pictures at later time points were taken under a blue filter to avoid confusing the bright light microscopy with the fluorescent microscopy. At 36 hours post infection, more epicenters of green were observed, indicating the spread of the virus (Figure 11). Interestingly, at 48 hours post infection, there appeared to be little activity (Figure 12). This may, however, be attributed to a slightly longer fixation time of forty eight hours that occurred due to technical difficulties with the fluorescent scope during this time period. The same spread seen at 36 hours post infection was apparent again at 60 hours post infection (Figure 13), but the biggest changes came at 72 hours post infection. These cells showed massive viral spread among the different epicenters of infection, with large masses congregating together (Figure 14).

Figure 10. SH-SY5Y Cells Infected with RVFV-GFP 24hpi

SH-SY5Y cells were infected with a GFP-tagged RVFV and stopped at 24 hours post infection. The cells were fixed with 4% PFA, and then imaged for fluorescence after a 24 hour fixation period. The images on the left are under bright light microscopy with a green filter, while the images on the right are of the same location but under green fluorescence detection. The lack of fluorescence indicates a lack of viral detection. All images were taken at 10x magnification.
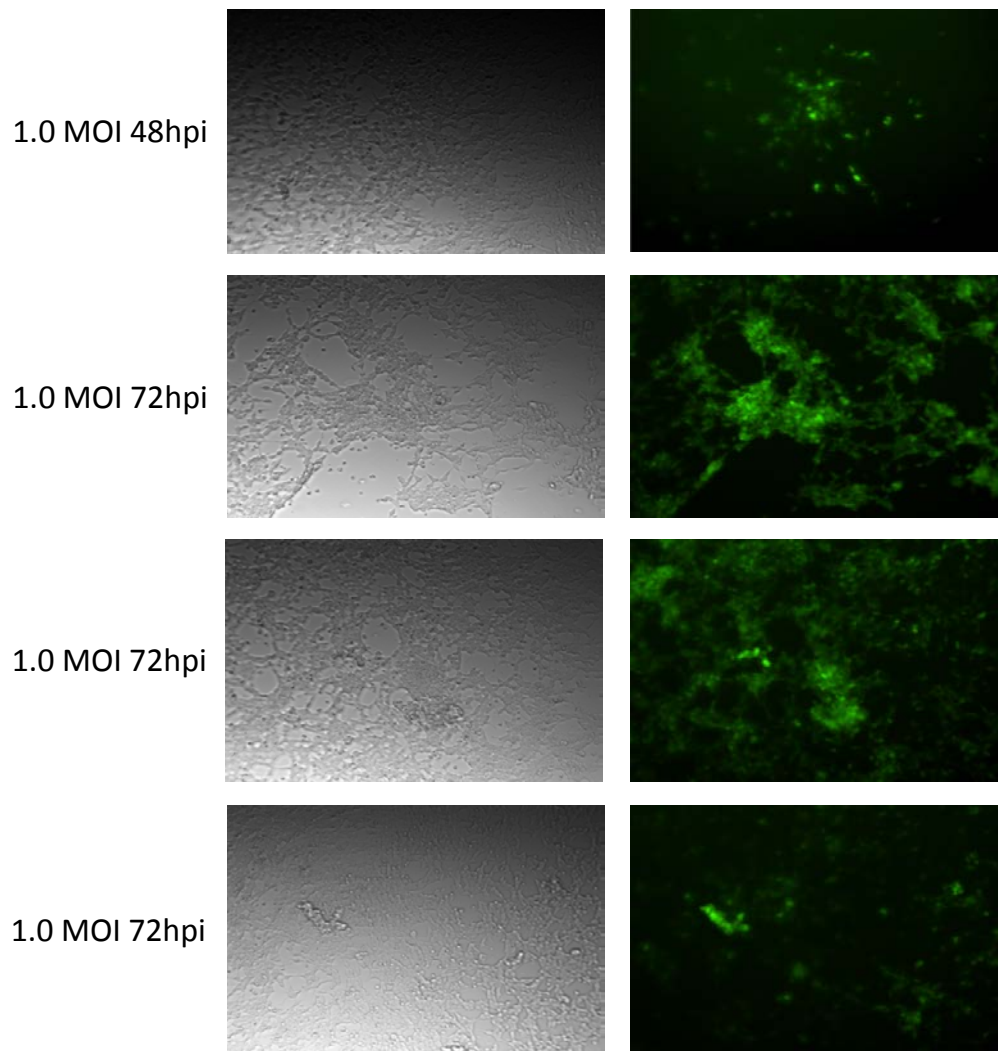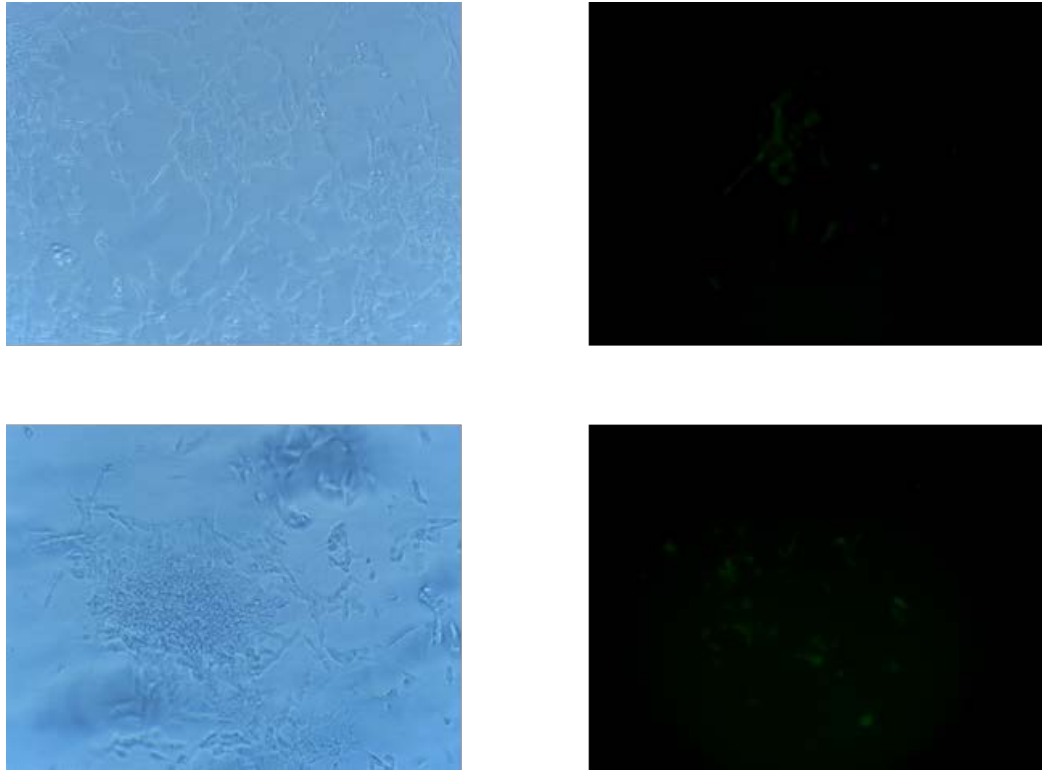
Figure 11. SH-SY5Y Cells Infected with RVVF-GFP 36hpi

SH-SY5Y cells were infected with a GFP-tagged RVFV and stopped at 36 hours post infection. The cells were fixed with 4% PFA, and then imaged for fluorescence after a 24 hour fixation period. The images on the left are under bright light microscopy, while the images on the right are of the same location but under green fluorescence detection. The lack of fluorescence indicates a lack of viral detection. All images were taken at 10x magnification.
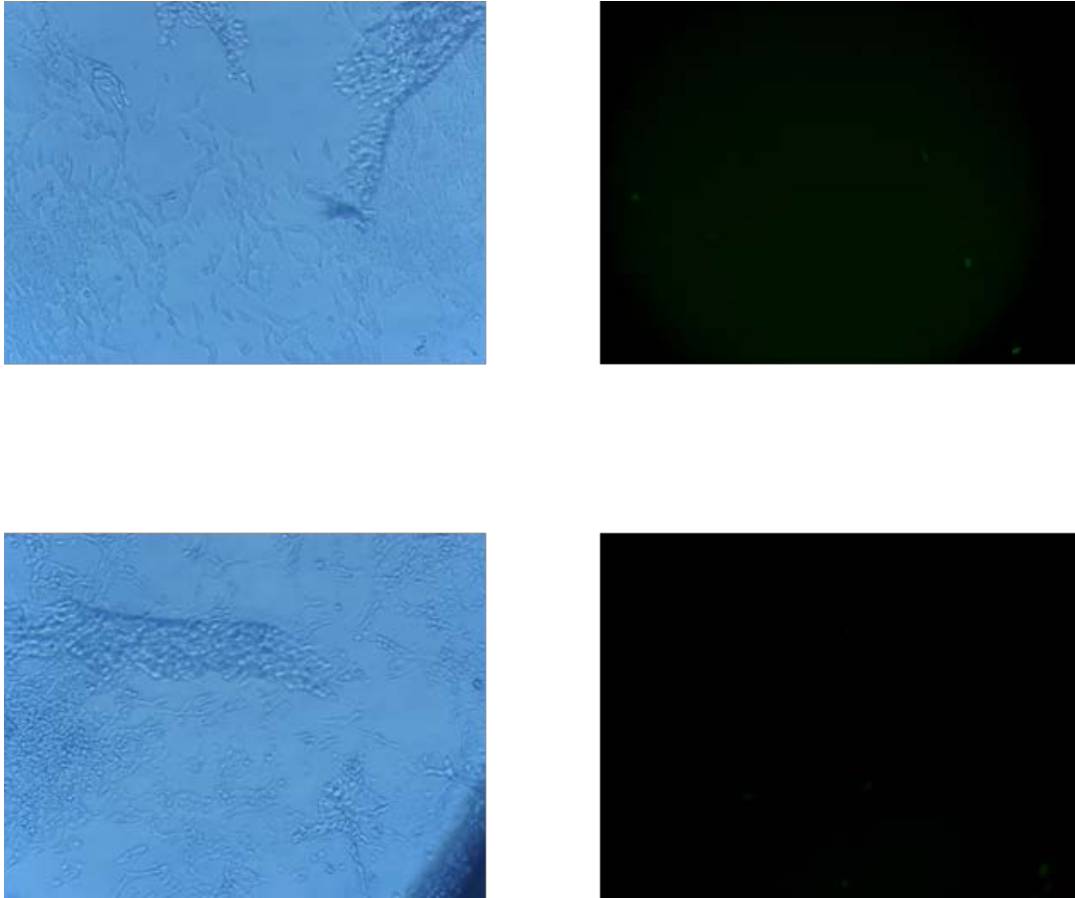
Figure 12. SH-SY5Y Cells Infected with RVFV-GFP 48hpi

SH-SY5Y cells were infected with a GFP-tagged RVFV and stopped at 48 hours post infection. The cells were fixed with 4% PFA, and then imaged for fluorescence after a 24 hour fixation period. The images on the left are under bright light microscopy with a blue filter, while the images on the right are of the same location but under green fluorescence detection. The lack of fluorescence indicates a lack of viral detection. All images were taken at 10x magnification.
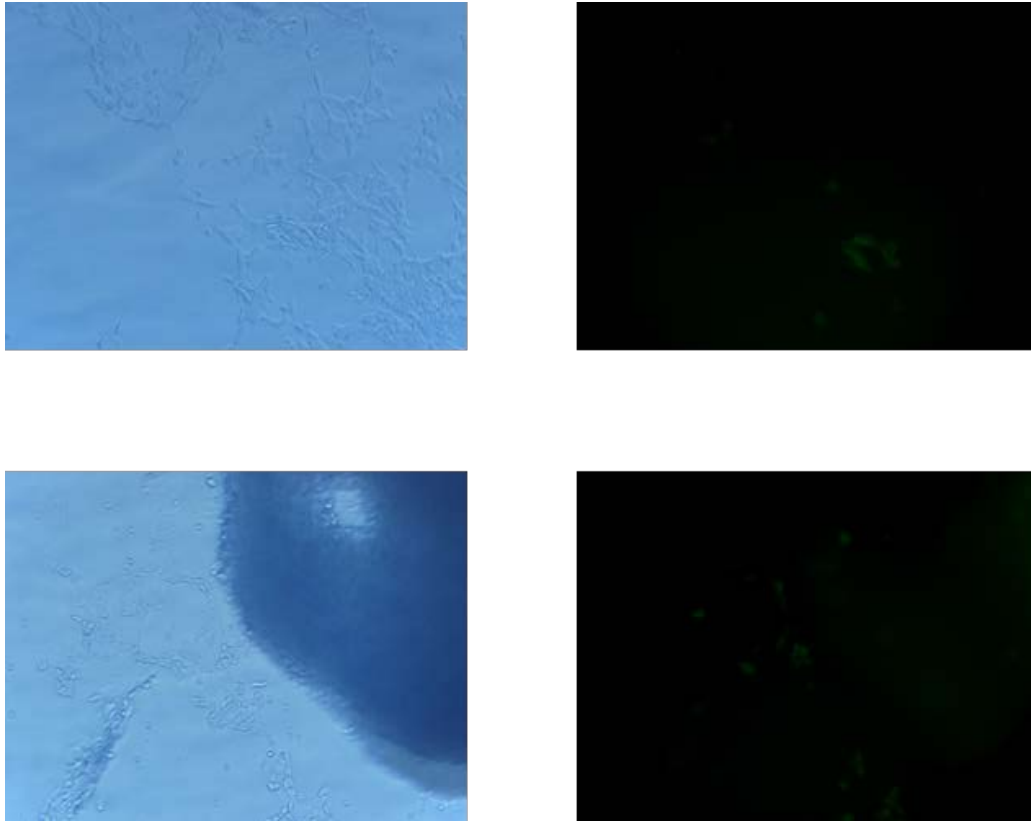
Figure 13. SH-SY5Y Cells Infected with RVFV-GFP 60hpi

SH-SY5Y cells were infected with a GFP-tagged RVFV and stopped at 60 hours post infection. The cells were fixed with 4% PFA, and then imaged for fluorescence after a 24 hour fixation period. The images on the left are under bright light microscopy with a blue filter, while the images on the right are of the same location but under green fluorescence detection. The lack of fluorescence indicates a lack of viral detection. All images were taken at 10x magnification.
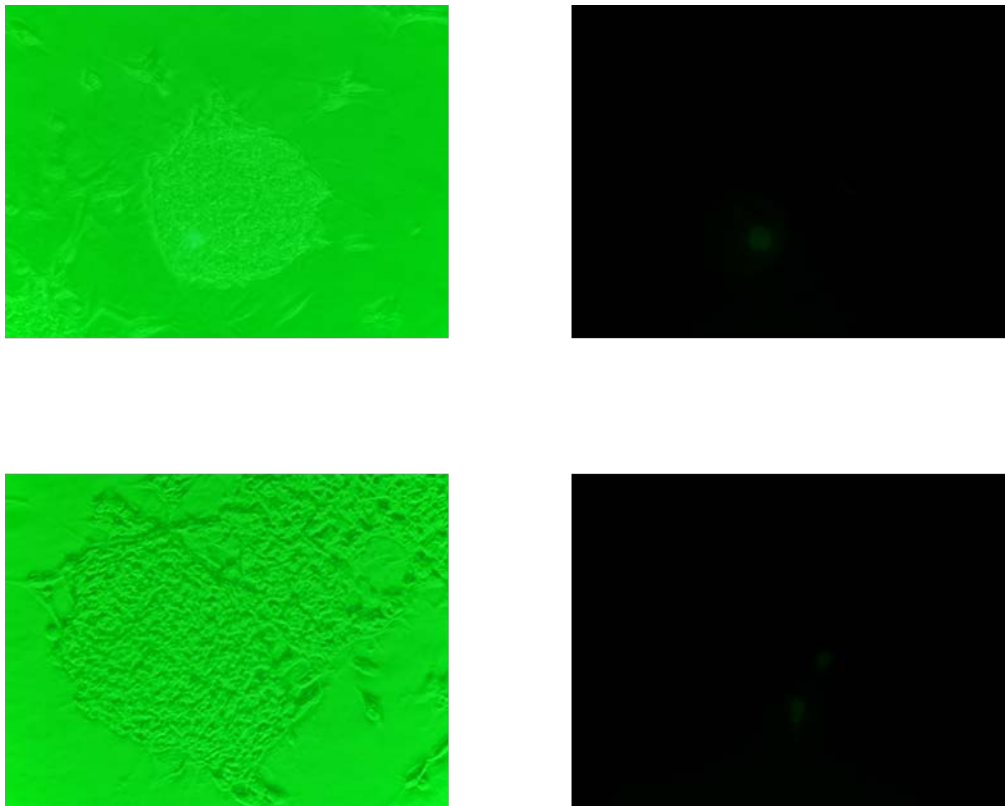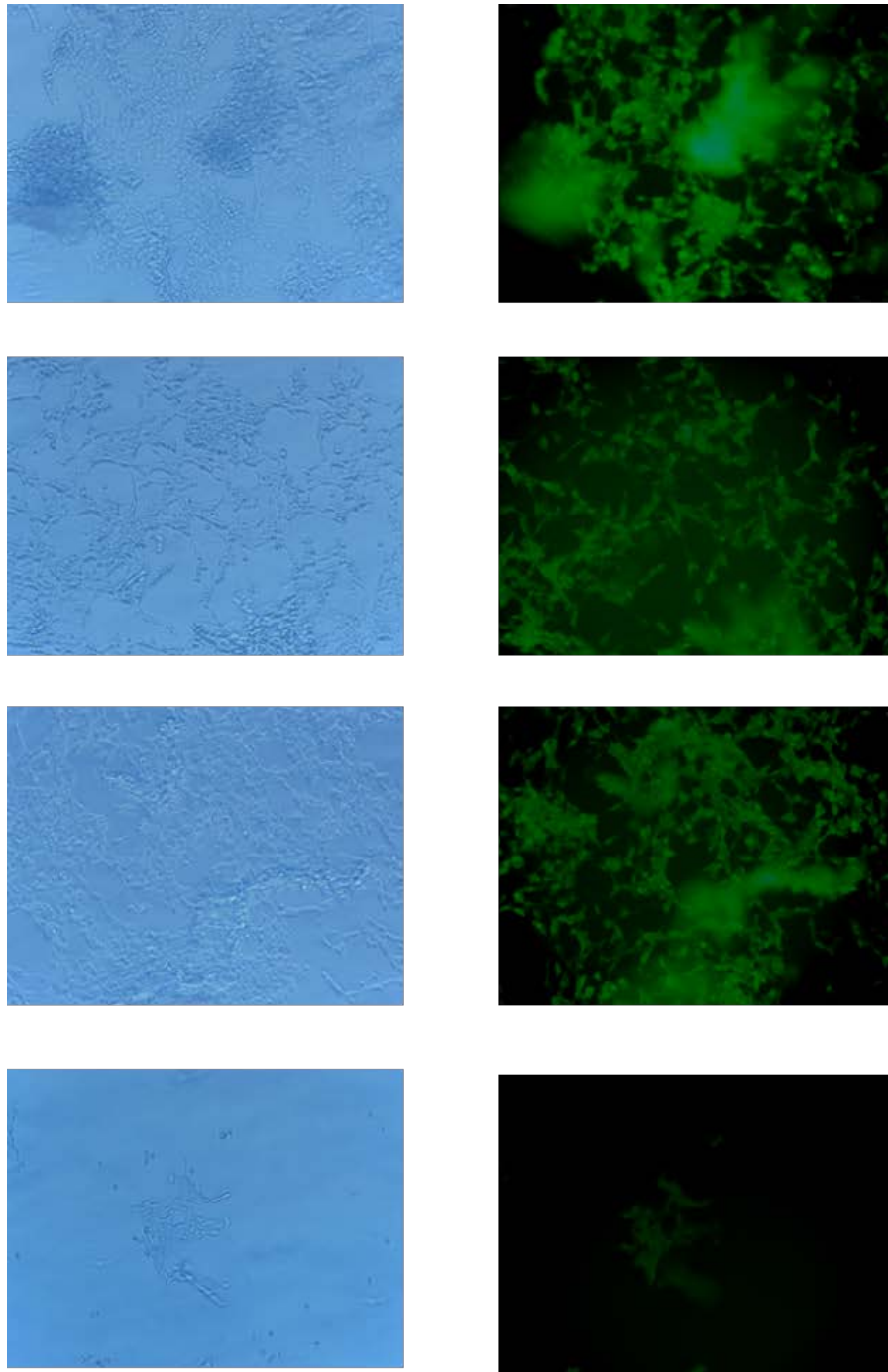
Figure 14. SH-SY5Y Cells Infected with RVFV-GFP 72hpi

SH-SY5Y cells were infected with a GFP-tagged RVFV and stopped at 24 hours post infection. The cells were fixed with 4% PFA, and then imaged for fluorescence after a 72 hour fixation period. The images on the left are under bright light microscopy with a blue filter, while the images on the right are of the same location but under green fluorescence detection. All images were taken at 10x magnification.

HBMEC cells provided by Dr. Carolyn Coyne were grown in both a 2D and 3D format before they were given to our lab for infection with Rift Valley Fever Virus (26). The 2D format, grown as a typical monolayer, appeared somewhat similar to Vero E6 cells but with more irregularities. Some appeared circular, while others had a few oblong portions, but for the most part were in an ovular shape. When infected, these cells showed immediate signs of morphological change at both 0.1 (Figure 15) and 1.0 MOI (Figure 16). The cells began rounding up in a more perfect circle and although they never came off the flask, they did appear to detach themselves a little bit from the monolayer as they were able to sway back and forth when the flask was moved. By 48 hours post infection, aggregate clumps were seen that did eventually detach from the monolayer by 72 hours post infection. The 3D format of these cells, on the other hand, behaved much differently. These cells were grown on a spherical latex bead, and showed similar morphological changes between the 0.1 (Figure 17) and 1.0 MOI (Figure 18) infections. At first, the beads mostly remained separated from one another, occasionally but rarely joined by a cell that grew between both beads. At 36 and 48 hours post infection, these beads were on top of one another. The cells appeared to merge most of them together, while some beads even showed signs of sheering the cells off altogether (Figure 18; 1.0 MOI 36hpi). Curiously, by 72 hours post infection, these aggregated beads appeared to separate themselves again, albeit with a few noticeable clearings where the cells had come off. The supernatants of these infections were collected at each MOI and time point indicated, and tested for viral titer by plaque assay (Figure 19). The 2D model of cells showed a steady exponential increased, while the 3D model appeared to have an increase followed by a decrease midway through the infection. Overall, the 2D HBMEC cells produced a higher titer than their 3D counterparts.
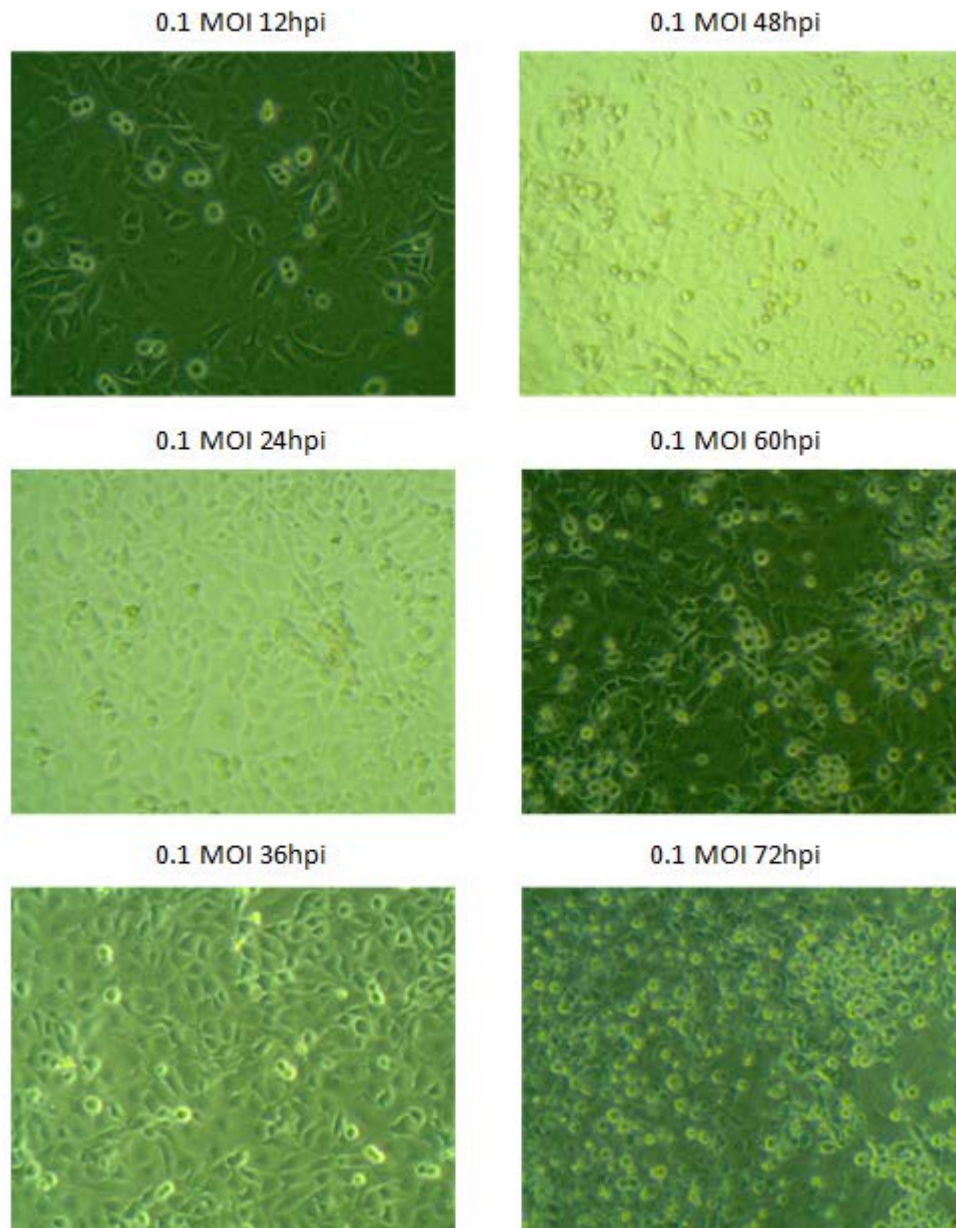
Figure 15. 2D HBMEC Cells Infected at 0.1 MOI

HBMEC cells grown in a 2D monolayer format were infected with RVFV ZH501 at 0.1 MOI, and imaged every twelve hours starting at 12 hours post infection and ending at 72 hours post infection. All images were taken at 20x magnification.
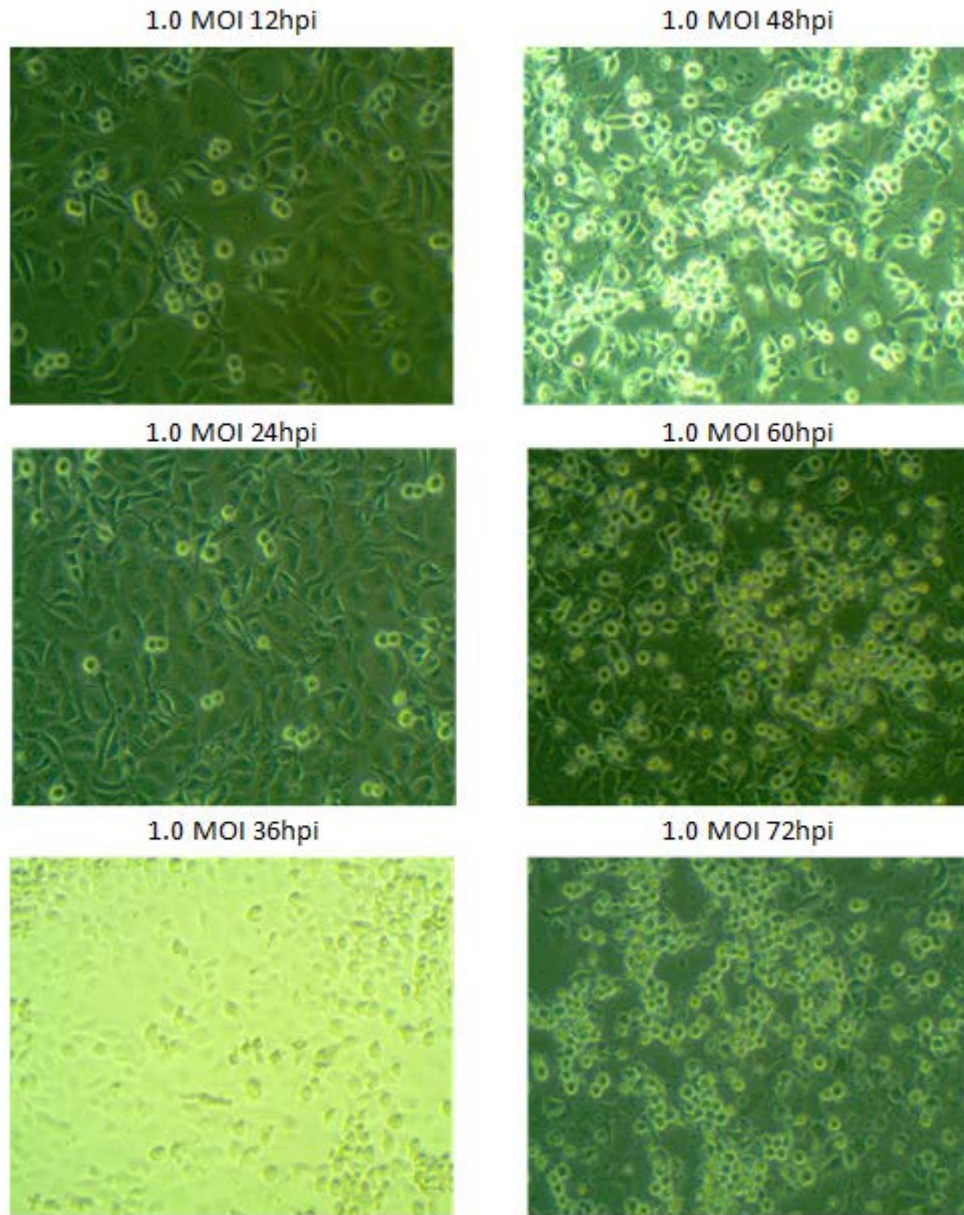
Figure 16. 2D HBMEC Cells Infected at 1.0 MOI

HBMEC cells grown in a 2D monolayer format were infected with RVFV ZH501 at 1.0 MOI, and imaged every twelve hours starting at 12 hours post infection and ending at 72 hours post infection. All images were taken at 20x magnification.
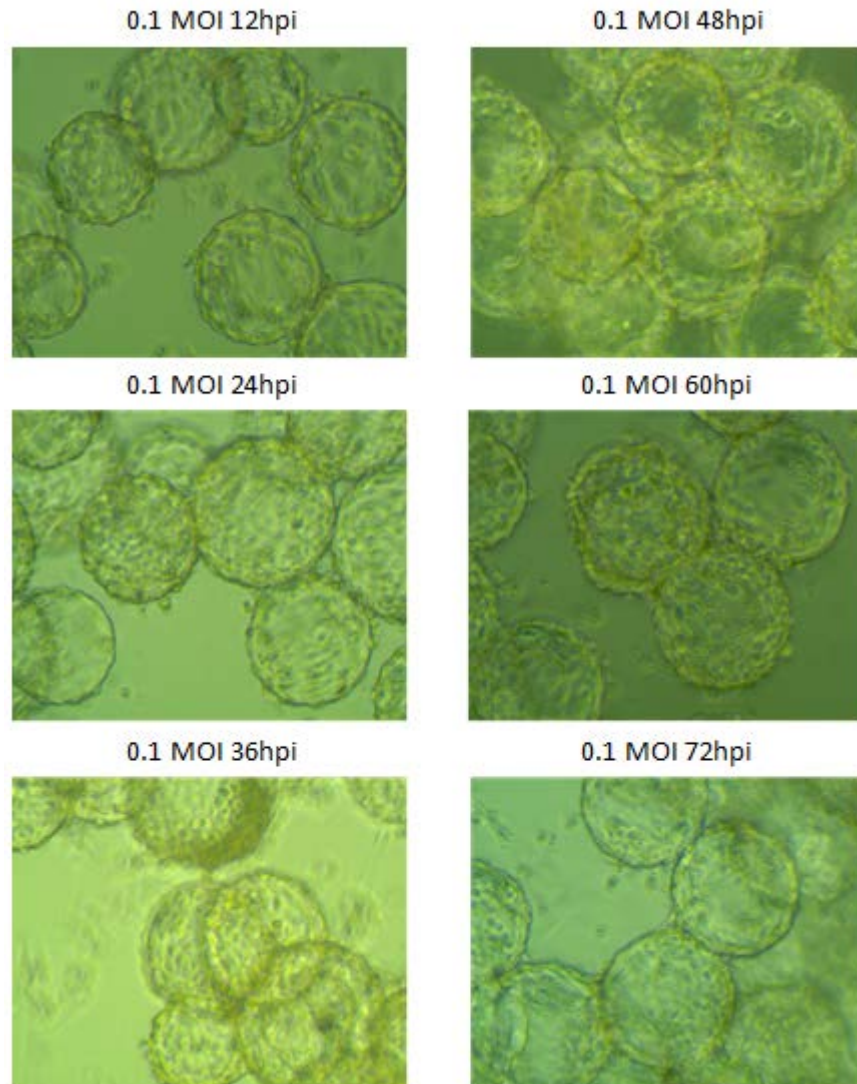
Figure 17. 3D HBMEC Cells Infected at 0.1 MOI

HBMEC cells grown in a 3D format on latex beads were infected with RVFV ZH501 at 0.1 MOI, and imaged every

twelve hours starting at 12 hours post infection and ending at 72 hours post infection. All images were taken at 20x

magnification.
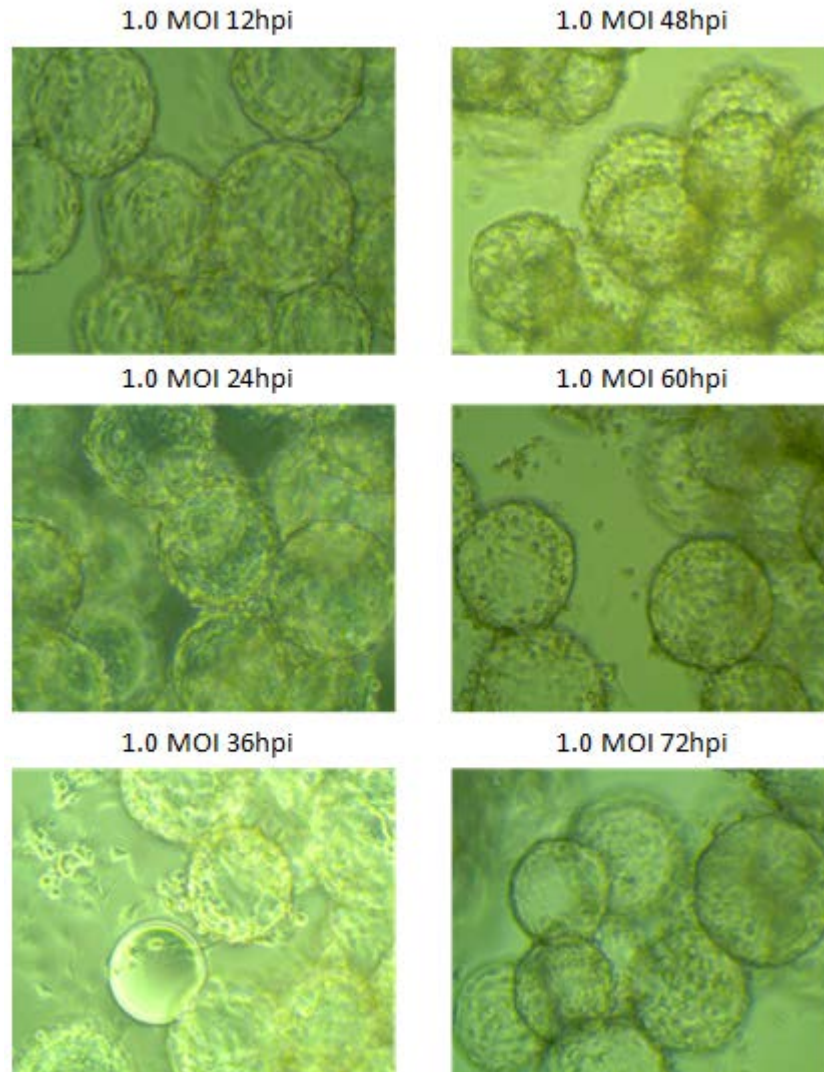
Figure 18. 3D HBMEC Cells Infected at 1.0 MOI

HBMEC cells grown in a 3D format on latex beads were infected with RVFV ZH501 at 1.0 MOI, and imaged every twelve hours starting at 12 hours post infection and ending at 72 hours post infection. All images were taken at 20x magnification.
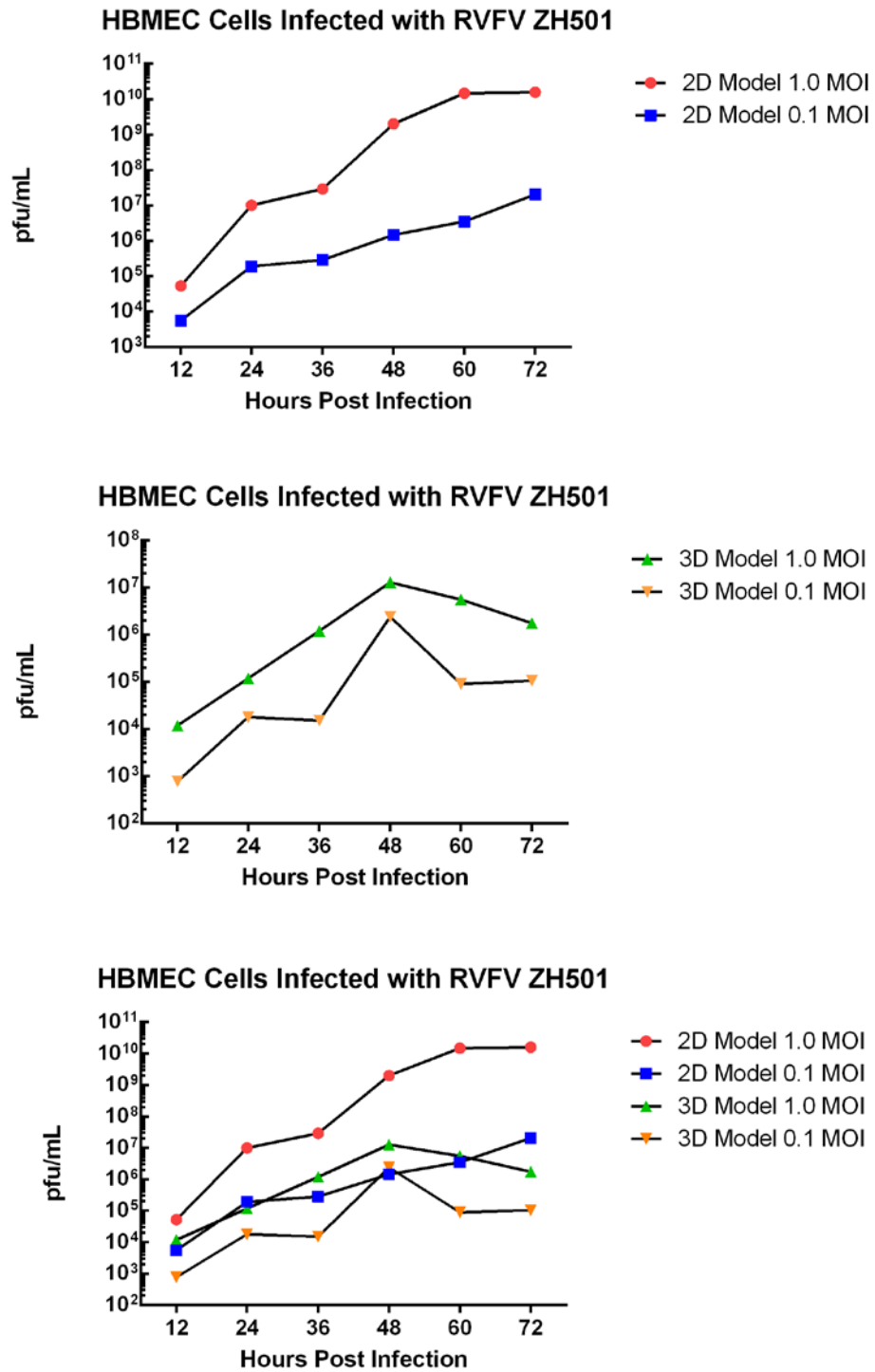
Figure 19. RVFV ZH501 Viral Growth in HBMEC Cells

Supernatants were taken from each HBMEC infection setup and tested for RVFV ZH501 viral growth at the time

points indicated. All viral quantification was performed via plaque assays.

50

4.2 AIM 2: COMPARE CYTOKINE/CHEMOKINE PRODUCTION FROM *IN VITRO* CELL LINE MODELS TO *IN VIVO* RAT INFECTIONS

Lewis rats uniformly develop lethal encephalitis disease when exposed to Rift Valley Fever Virus by aerosol (27). Clinical disease is associated with visible signs that start around day five post infection, and include things such as head tilting, circling in the cage, unresponsive to stimuli, and/or perforin staining around the nose (27). Death typically occurs six to eight days after infection. Significant pathology within the brain of aerosol RVFV-infected Lewis rats has been documented by our laboratory (27). Physiological changes within the rats occurring prior to the onset of clinical signs, such as a cytokine storm, have yet to be fully understood.

In previous Lewis rat experiments performed in our lab, the cytokines and chemokines GRO-Alpha, IFN-Alpha, IFN-lambda, IL-8, MCP-1, M-CSF, and RANTES were all significantly increased in expression in the brain tissue of rats with encephalitis (27). In order to determine whether *in vitro* infection of SH-SY5Y and HBMEC cells induced cytokine expression that is similar to that seen in infected rats, the supernatants from the experiments described in Aim 1 were tested using a multiplex containing these analytes. Values were reported in pg/mL, and at 12 and 72 hours post infection to represent the changes seen over the course of infection (Figure 20). HBMEC cells in both the 2D and 3D formats showed dramatic cytokine dysregulation in all of the tested analytes. SH-SY-5Y cells, however, did not show this same dysregulation in all of the analytes. Interferon levels were minimal or nonexistent in both cell lines. All materials were still infectious at the time of testing to ensure the preservation of all cytokines and chemokines that may have otherwise been destroyed during an inactivation procedure.

3D HBMEC 1.0 MOI

2D HBMEC 1.0 MOI

SH-SY5Y 1.0 MOI
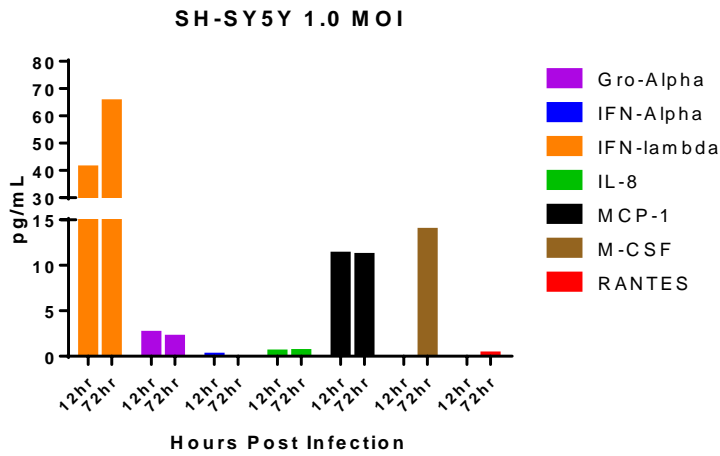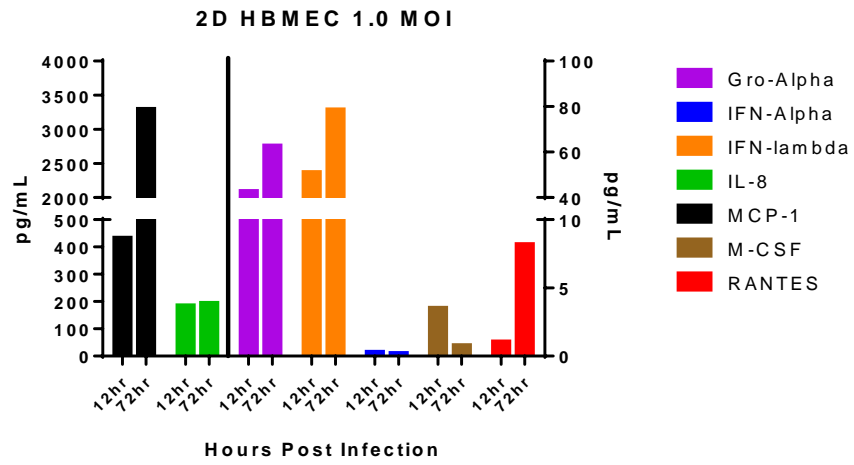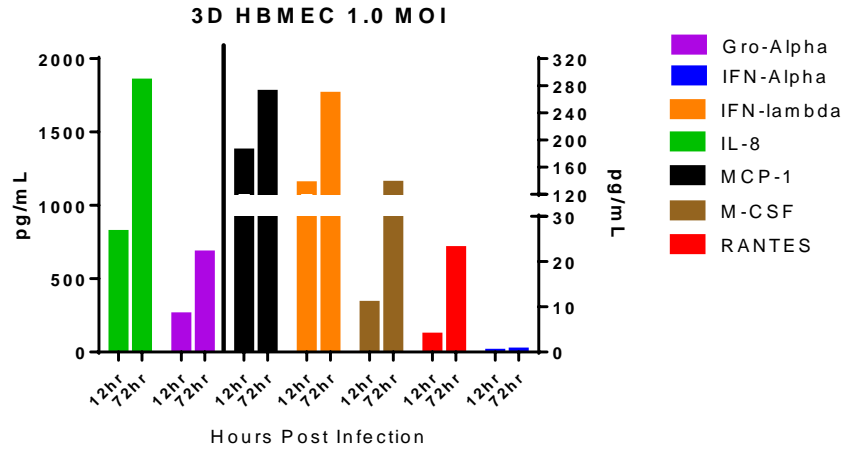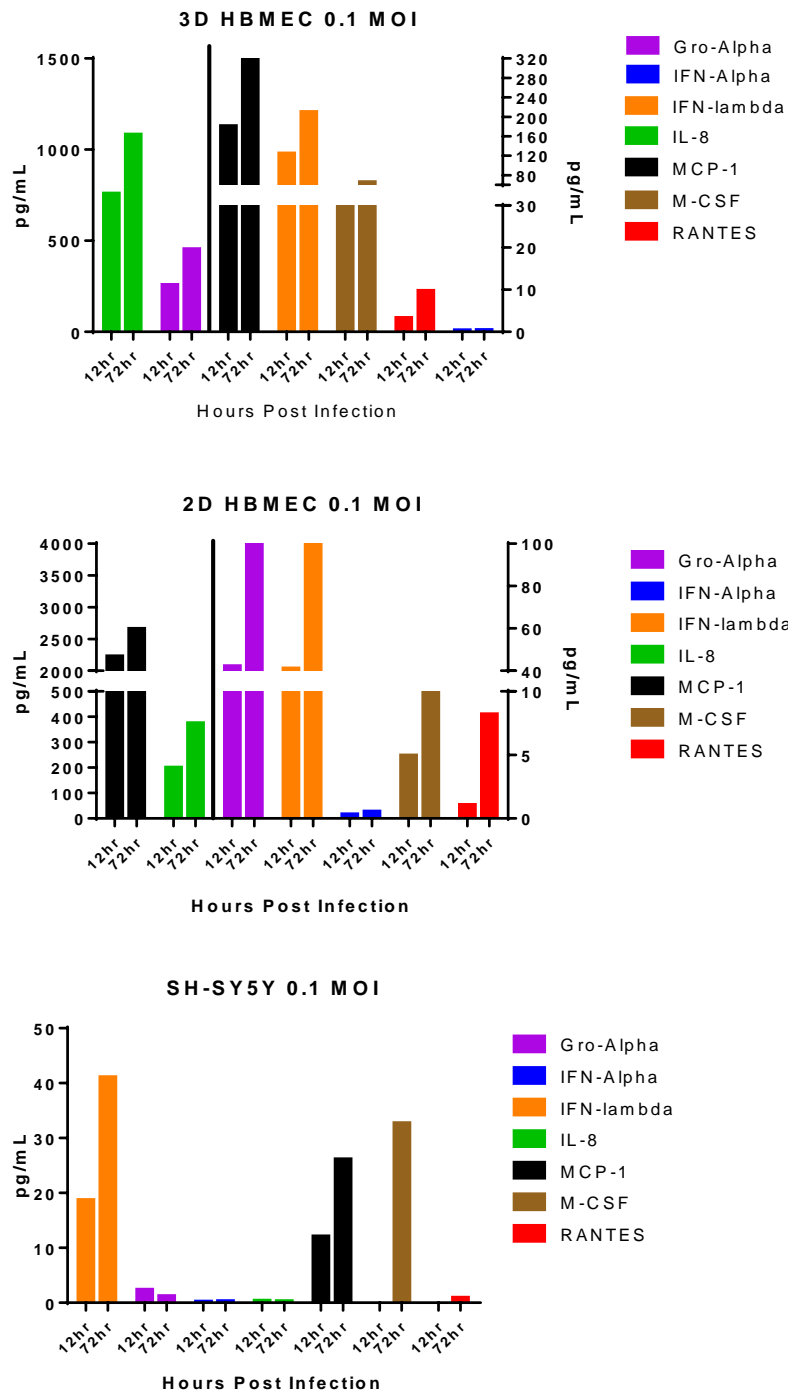
Figure 20. Cytokine and Chemokine Response in SH-SY5Y and HBMEC Cells

SH-SY5Y and HBMEC cells were tested with a multiplex ELISA for the presence of GRO-Alpha, IFN-Alpha, IFN-lambda, IL-8, MCP-1, M-CSF, and RANTES at various time points during RVFV ZH501 infections at the MOI indicated.

In addition, MMP-9, a protein associated with the breakdown of the blood-brain barrier, was tested for its presence in the whole brain of serial sacrificed Lewis rats after exposure to aerosolized Rift Valley Fever Virus (Figure 21). These samples were homogenized and tested on an ELISA plate, ranging from uninfected controls to nine days post infection. Significance at the $p < 0.05$ range was found at day 3 post infection, as well as days 5 and beyond. To look more specifically within the brain, just the cortex was homogenized from a second experiment of Lewis rats that were again infected with aerosolized RVFV (Figure 22). These samples ranged from uninfected controls to six days post infection. Significance at the $p < 0.05$ level was found on days 3, 5, and 6 post infection. Finally, to assess circulating MMP-9, the serum was tested on these same rats for the presence of the protein (Figure 22). Significance at the $p < 0.05$ level was only found here at day 3 post infection.
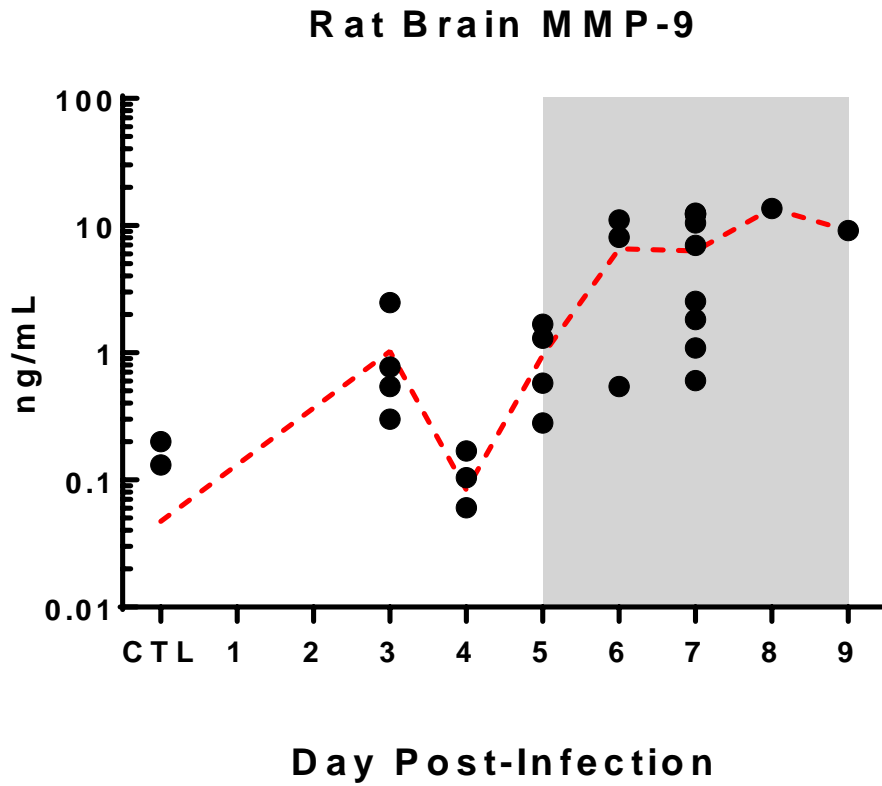
Figure 21. MMP-9 Presence in the Whole Brain of Infected Lewis Rats

A MMP-9 ELISA was run on whole brains extracted from Lewis rats infected with RVFV ZH501 and serial sacrificed from zero to nine days post infection. The shaded region indicates the window of clinical disease.
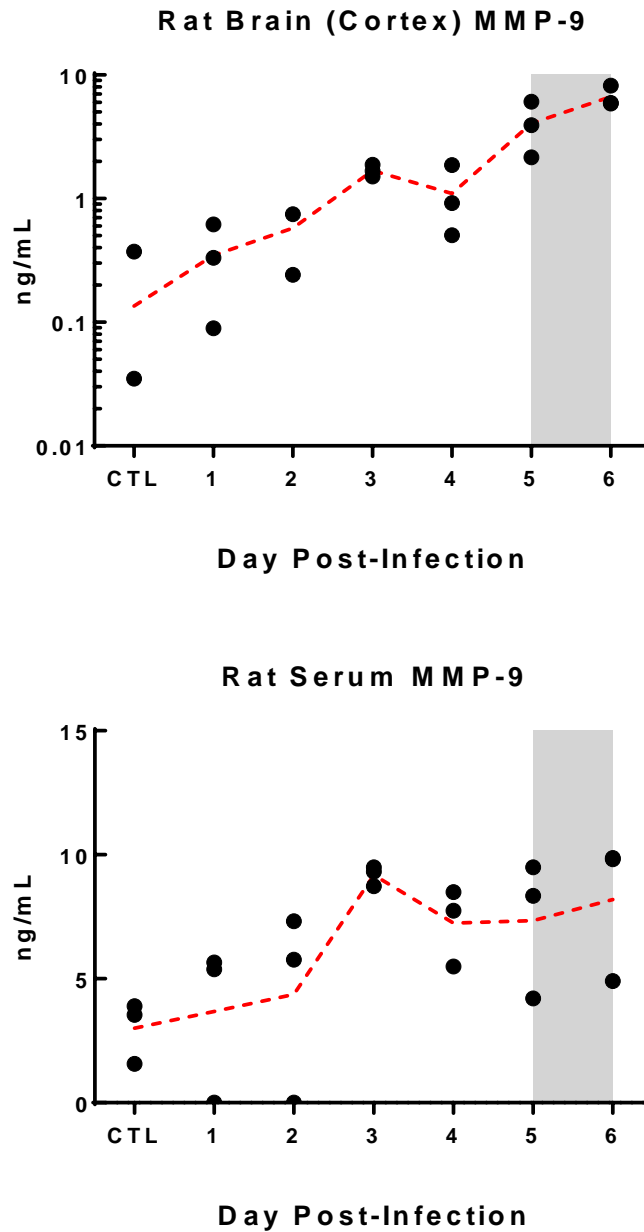
Figure 22. MMP-9 Presence in the Cortex and Serum of Infected Lewis Rats

A MMP-9 ELISA was run on cortex of the brains extracted as well as the serum from Lewis rats that were infected with RVFV ZH501 and serial sacrificed from zero to nine days post infection. The shaded region indicates the window of clinical disease.

4.3 AIM 3: IDENTIFICATION OF THE PATHWAY OF NEUROTROPIC DISEASE IN LEWIS RATS

One of the overarching goals of our lab is to determine the route of neuroinvasion of RVFV in Lewis rats. Our predominant theory is that during aerosolized infection with RVFV, the virus travels from the olfactory epithelium to the olfactory bulb of the brain. Early work has indicated that the virus enters the brain quickly during infection, which suggests that it takes a direct route there (27). To determine the timing of virus emergence in various components of the CNS, Lewis rats were infected by aerosol and serial sacrificed out to six days post infection. At each day, the brain and various organs were extracted for viral testing by PCR. Our previous work has shown the virus infects the lungs, liver, and spleen in high titers (27). However, while testing the organs harvested, the cervical lymph nodes showed surprising amounts of virus and as such were included alongside the brain portions tested (Figure 23). An early spike was seen in the cervical lymph nodes above the levels seen in the brain, whereas the viral titers in the brain exponentially grew larger as the infection went on. The first section of the brain to show viral emergence was the olfactory bulb and cortex on day two post infection, then followed by the other CNS tissues at day three post infection. These early detections of virus are well before the clinical signs of disease develop at five days post infection.
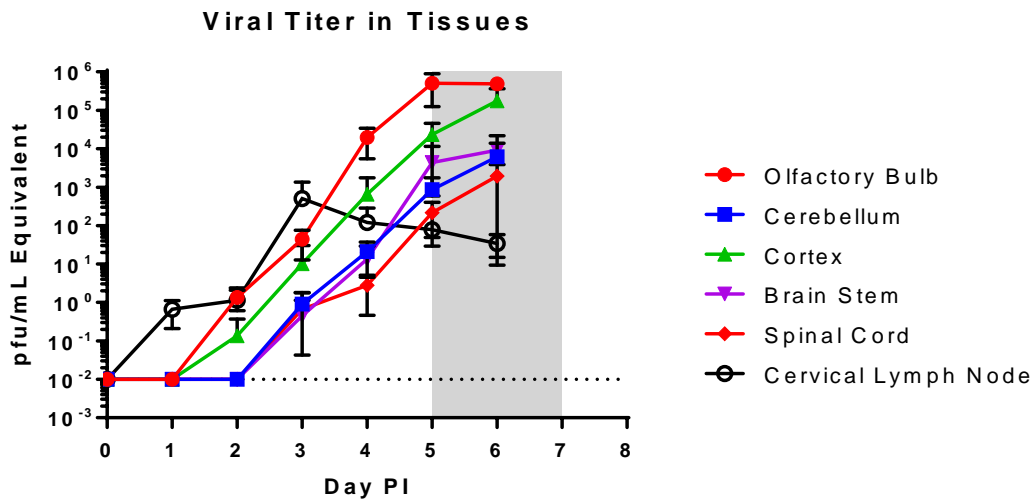
Figure 23. Viral Titers in Lewis Rat Tissues after RVFV Infection

Lewis rats were infected with RVFV ZH501 by aerosol at a dose of 1×10^3 pfu/rat, and serial sacrificed from zero to six days post infection. PCR was performed in the selected tissues for the presence of virus. The shaded region indicates the window of clinical disease.

Interestingly, a higher dose of RVFV by aerosol showed a slightly different result. In a new experiment, a high dose of 1×10^4 pfu/rat was given to each rat and the tissues were harvested similarly for viral testing by PCR (Figure 24). When exposed to a high dose, RVFV was found in all of the brain tissues tested at one day post infection. This supports the idea further that the virus enters the brain first during infection by aerosol.

Viral Titer in Tissues at 2×10^4 pfu/rat
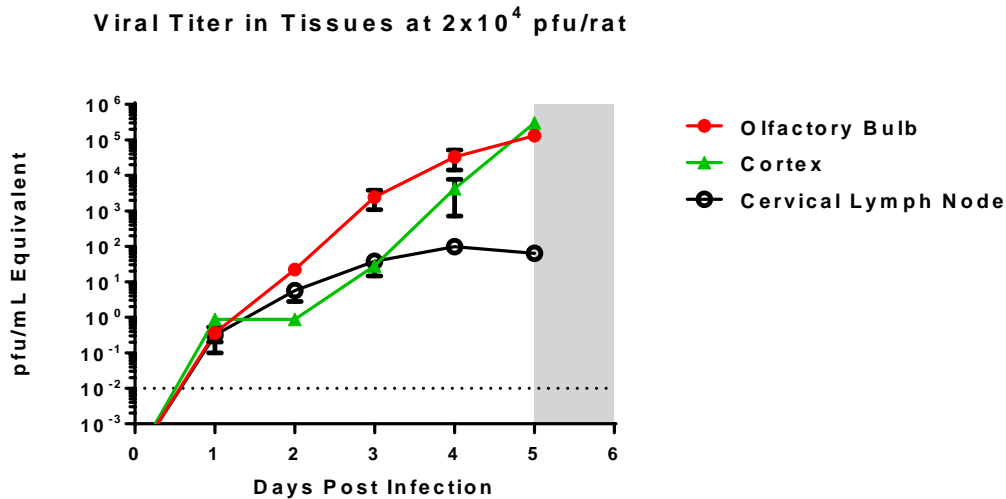
Figure 24. Viral Titers in Lewis Rat Tissues after High Dose RVFV Infection

Lewis rats were infected with RVFV ZH501 by aerosol at a dose of 2×10^4 pfu/rat, and serial sacrificed from zero to six days post infection. PCR was performed in the selected tissues for the presence of virus. The shaded region indicates the window of clinical disease.

Next, the blood brain barrier permeability during infection was assessed through the use of FITC salt. This was performed to test the theory that the virus may cross the blood brain barrier to gain entry into the brain rather than going through the olfactory epithelium. Again, Lewis rats were infected by aerosol and serial sacrificed out to day six post infection. Two minutes before sacrifice, the FITC salt was injected by tail vein and allowed to circulate within the body. Then, the serum, brain, and spinal cord were all harvested and measured for fluorescence from the FITC salt within them. These values were then normalized to each rat's individual fluorescence in the serum to provide a base line, and graphed together (Figure 25). A trend can be seen that spikes upward between days 4 and 5 post infection, which correlates with the onset of clinical disease. This suggests that there may be a breakdown of the blood brain barrier later rather than during initial infection.

59
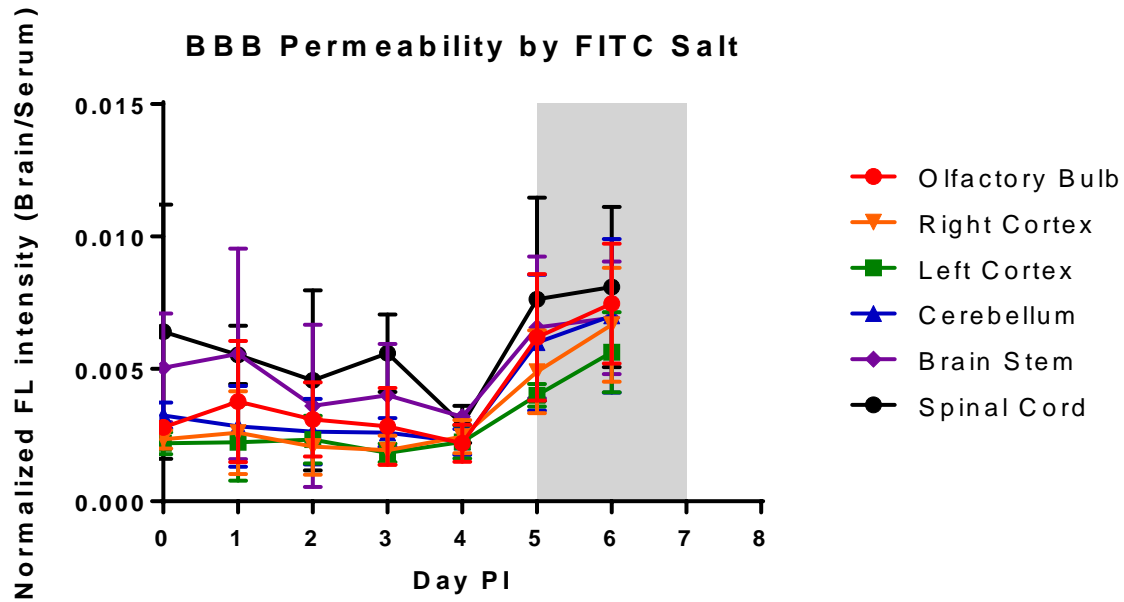
Figure 25. FITC Salt Intensity in Lewis Rat Tissues after Infection

Lewis Rats infected with RVFV ZH501 were tail vein injected with FITC salt before being sacrificed for tissue extraction. Tissues were tested using a FITC salt extraction and normalized to each animal's serum FITC salt levels. The shaded region indicates the window of clinical disease.

To further test the permeability of the blood brain barrier, an agent for imaging in live animals was used during a time course infection. Lewis rats were infected by aerosol with RVFV and left unaltered until day 4 post infection. At this time, Superhance 680 was injected by tail vein and allowed to circulate throughout the body in both the infected rats and a set of uninfected control rats. Superhance 680 is a small molecular weight (1540 g/mol) imaging agent that is capable of passing through small breaks in the blood brain barrier into the CNS. Imaging for this agent used an excitation of 675nm with an emission of 692nm. At 24 hours post injection, 5 days post infection, the rats were imaged live (Figure 26). The total flux calculated based on how much of the reagent made it into the brain showed a significant difference between the uninfected and infected at a value of p=0.052. At 48 hours post injection, 6 days post infection, the total flux had a significant difference at p=0.016. After this, the brains were

60

removed from both the uninfected and the infected and imaged ex vivo. Although these images were not measured for total flux, there is a clear difference between the images by color variation.
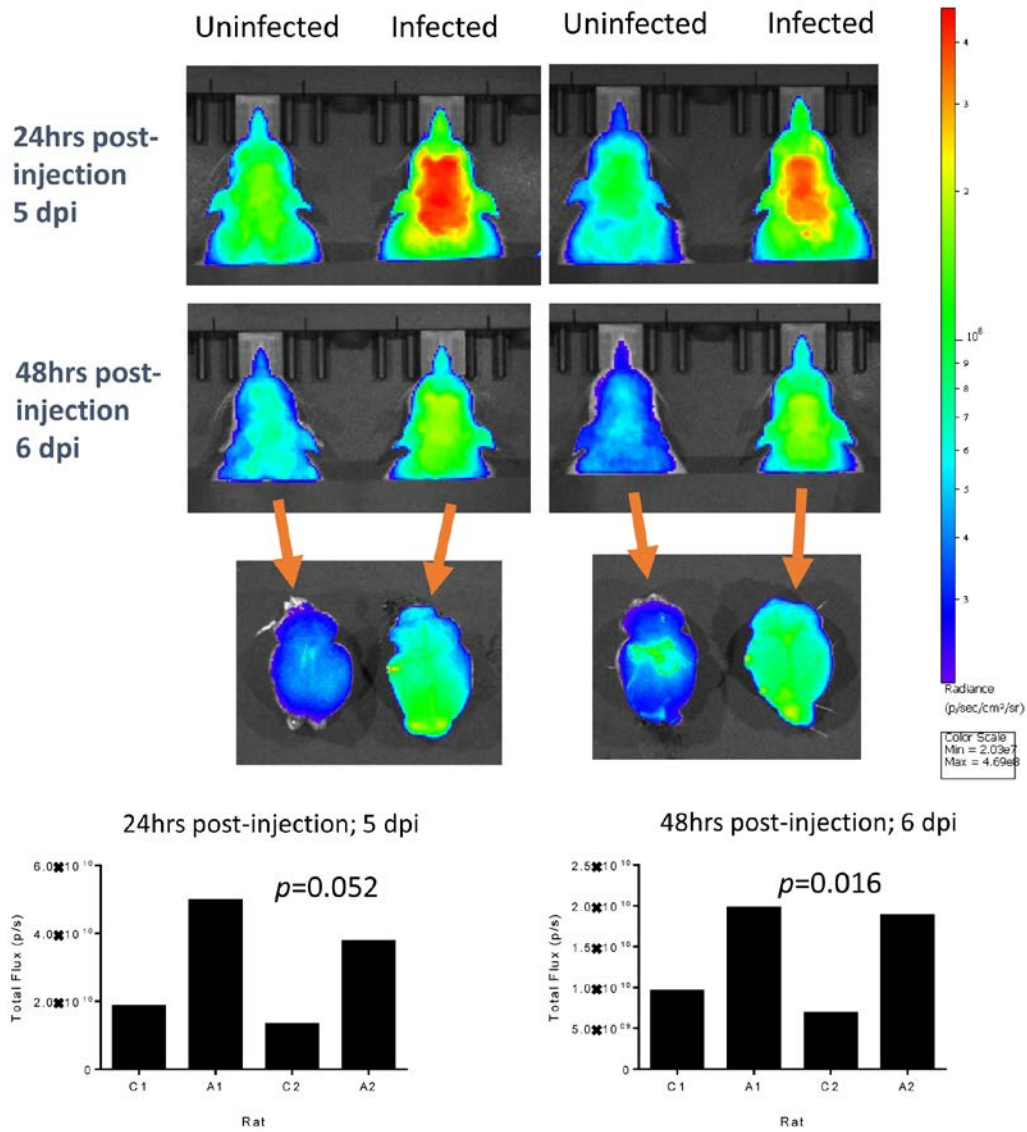
Figure 26. IVIS Imaging of RVFV Infected Lewis Rats

RVFV ZH501 infected rats were injected with Superhance 680 at four days post infection, and imaged in vivo 24 and 48 hours later to assess for blood brain barrier permeability. The brains were extracted at 48 hours post injection and imaged ex vivo.

5.0   DISCUSSION

Rift Valley Fever Virus is an important arbovirus that has swept throughout Africa and into the Arabian Peninsula leaving destruction everywhere it touches. Outbreaks lead to severe disease and death in ruminants, and can infect humans causing symptoms ranging from a febrile illness to major complications including encephalitis that may lead to death. RVFV is listed as a Category A pathogen and an overlap Select Agent, recognized for the threat it presents both in bioterrorism and natural spread. Understanding the neuropathogenesis of the virus is a driving force behind the research of the encephalitic form of the disease for possible therapeutics or vaccines down the road.

It is vital to have a good model for both in vitro and in vivo work when studying any disease that cannot be ethically replicated in humans. At this time, a rodent and non-human primate model have been well developed by our lab that consistently replicates the encephalitic disease caused by RVF, using Lewis rats and African Green Monkeys (4), (27). However, no such model exists for in vitro work which would ultimately be start for toxicity and efficiency testing of therapeutics.

Vero E6 and BHK-21 cells, the two cell lines commonly used in the propagation of RVF, grew different morphologically from both the SH-SY5Y cells and each other. All three cell lines had their own unique characteristics. Vero E6 cells grew in a cobblestone fashion, BHK-21 cells were long and striated, and SH-SY5Y cells grew spindly with filaments coming off of the ends.

However, when infected with Rift Valley Fever Virus, they all exhibited cytopathic effect (CPE). The cells in each infection began to clump together, and rounded up into a spherical shape. Visually, these cells would be difficult to distinguish in the late infection; around 72 hours post infection, when their original morphology was lost. The only major difference was the massive clumping shown by SH-SY5Y cells in these later time points. All three of these cell lines were infected at 0.1 and 1.0 MOI to ensure that there was enough virus for replication, and at the same time not too much to cause viral interference. If a MOI is too low, then an infection may not properly be initiated. If a MOI is too high, then there will be too many viral particles attempting to enter the cells and they will infect every cell in the flask, leading to mass cell death with no cells available for the second round of replication, effectively ending the infection after the first entry.

Viral titers from these three infected cell lines needed to be assessed to determine the permissivity of them. Although they shared similar morphology after infection, the amount of virus produced by the cells was unknown. Vero E6 cells had the highest viral titer immediately after infection than the other two cell lines, and maintained this until the 36 hour mark. SH-SY5Y cells, on the other hand, had the lowest initial viral titers of all the cell lines. These cells however exhibited exponential growth throughout the entirety of the infection, whereas Vero E6 and BHK-21 cells were slow to start, had an explosion of growth between 36 to 48 hours post infection, and then leveled off again. At the end of infection, at the 72 hour post infection mark, all three cell lines were within a log of their respective MOI. This proves that SH-SY5Y cells were just as permissive to infection as their counterparts, albeit with a slightly different viral growth pattern.

Vero E6 cells and BHK-21 cells have defective antiviral properties that make them prime candidates for infection by a variety of viruses, such as Rift Valley Fever. This makes the similar permissivity of the SH-SY5Y cells intriguing since there is no known similar defect in these cells. Although further testing is needed, this suggests that RVFV has a mechanism built into it to specifically counter the antiviral properties of neurons, which is supported by the encephalitic disease shown during infection in animal models. The virus was not only able to replicate easily, but was able to reach extremely high titers.

In an attempt to gain further insight into the changes that took place in the SH-SY5Y cells, the RVF-GFP virus was used to infect them and observed for viral growth with a fluorescent microscope. The initial hope was to see where exactly in the cells the infection hit first, but the microscopes that were used were not quite powerful enough to provide that much detail. Instead, the foci of each infection were able to be seen using the microscope. Under live imaging, major areas of infection were able to be seen at 48 hours post infection that was otherwise not observable with the regular light microscope. Areas of clumping and rounding were green with fluorescence as expected, but cells that looked healthy also showed fluorescence. This indicates that morphology changes happen after infection is established in the cells, and not as an immediate reaction to viral entry. With this knowledge, RVF-GFP virus could prove to be useful in determining the route of infection using an *in vivo* model.

HBMEC cells are primary human brain microvascular endothelial cells that compose the blood brain barrier. They are capable of being grown in a monolayer and in a three dimensional format around a latex bead (26). These cells were used to see if RVFV was capable of infecting them, since the effects of this virus on the blood brain barrier is currently unknown. In the 2D format, which is essentially a monolayer, the cells had a large increase in viral titer immediately

after infection, which correlates to the early morphological changes observed. These cells then continued to create virus at high titers, ultimately reaching titers that were higher than Vero E6, BHK-21, and SH-SY5Y cells at the 1.0 MOI level. However, at 0.1 MOI the titer was significantly lower and actually ended at a lower point than the other three cell types at this MOI. This suggests that the amount of virus during initial infection plays a very big role in the outcome with HBMEC cells, which was not the case with the three other cell lines, all of whom ended with titers very near each other regardless of MOI. This system, unfortunately, did not account for factors such as sheering of cells that may occur in the body as fluids are rushing past the blood brain barrier cells. This could help to spread viral infection quicker, resulting in even higher viral titers and destruction.

To account for the fact that cells are not always in a perfect monolayer in the body, the HBMEC cells were grown on a latex bead that created a spherical 3D shape capable of infection from all angles. The 3D conformation may more accurately represent in vivo properties of the cells (26). These latex beads were grown in a suspension, allowing them to freely move rather than stick to the bottom of the flask. When infected, the cells showed a trend of increasing viral growth until 48 hours post infection, after which the viral titers began decreasing. This was also represented in the morphology. The cells in the 3D format appeared to merge the latex beads together as the cells themselves began clumping, but then interestingly began to separate again after 48 hours post infection. The cells never appeared to completely die out as in the other infections, suggesting that they may be more resilient to infection when in a 3D format.

Based off of previous data that our lab has published, specific cytokines and chemokines that are known to be dysregulated in Lewis rats during RVFV infection were tested for their presence in SH-SY5Y and HBMEC cells. These analytes included GRO-Alpha, IL-8, MCP-1,

M-CSF, RANTES (27). In addition, IFN-alpha, IFN-beta, and IFN-lambda were tested in the cell lines since they are known antiviral activators in a large variety of different cell times. Of these, the cells that were tested had no IFN-beta in them at any time point or MOI. Also, IFN-alpha appeared at either extremely low or nonexistent levels. Since interferons are related to an antiviral response, this helps to explain the permissivity for infection seen throughout the cells. It is proven here that there is indeed either a defect or complete lack of antiviral response in SH-SY5Y and HBMEC cells. However, each of the other analytes all appeared in some form during infection. In the Lewis rat experiment, each of these analytes showed an increase over time. Similarly, almost all of the analytes had an increase from 12 to 72 hours post infection. HBMEC cells showed the greatest comparability to the *in vivo* rat data, with all of the analytes having a larger output at 72 hours post infection. SH-SY5Y cells only showed marked increases in IFN-lambda, MCP-1, and M-CSF. With this information, the HBMEC cells appear to be an ideal model for infection of the blood brain barrier. They mimic what is seen during *in vivo* infections, and are very permissible to infection. SH-SY5Y cells seem to be lacking a similar response as that seen in the Lewis rats. However, this could be attributed to the difference between species. With most of the analytes showing comparability, along with the high permissivity, the SH-S5Y5 cells prove to be a good model as well for the *in vitro* infection of neuronal cells.

Matrix metalloproteinase 9 (MMP-9) is a matrixin primarily responsible for the degradation of the extracellular matrix of cells. MMPs are regulated by various mechanisms such as direct transcription or inhibition by endogenous inhibitors, and are used in the degradation of old or dying cells marked for death. However, certain diseases or external influences can cause the delicate balance established to cause a massive influx of MMP, creating

problems for the cells it interacts with and the host itself. Since MMP-9 has been associated with the breakdown of the blood brain barrier in other viruses such as Japanese Encephalitis Virus (25), our lab began to pursue the theory that the same may happen during RVFV infection. When the presence of MMP-9 was tested in both the serum and brains of infected Lewis rats, MMP-9 levels were at very low levels in the brain until the clinical window of disease was reached. At this point, the MMP-9 titers skyrocketed to extremely high levels. Interestingly, the serum showed that there were fairly high levels even in the background of infection. However, at 5 days post infection, these levels spiked to high levels just like what was seen in the brain. One point that stood out from the rest was a significant increase at day 3 post infection in all of the tested samples, both serum and brain. This then dipped down against at day 4 post infection before increasing permanently at day 5 post infection. This increase may be associated with an early breakdown of the blood brain barrier, followed by the barrier closing back up, before being completely broken apart. This idea is supported by the morphology and viral titers observed in the 3D model of the HBMEC cells. It is also further supported by the increased levels of IFN-lambda found during infection of the cells *in vitro*. IFN-lambda is known to play a role in the tightening of the blood brain barrier, suggesting that the release of this interferon may help drive MMP-9 levels back down after an initial breakage in the barrier. The early increase followed by a decrease may occur because the cells are therefore able to regain their structure after initial infection. Further experiments would need to be conducted on the 3D model of HBMEC cells to see if during later time points the viral titers increase again, as the MMP-9 data suggests may happen.

Throughout the various experiments performed on the Lewis rat models, various portions of the brain as well as other various organs were harvested and tested for viral titer. By two days

67

post infection, virus was detectable in the olfactory bulb of the brain. At three days post infection, the entire brain showed viral replication, and continued to increase until the euthanization or death of the animal. Specifically, the olfactory bulbs remained the earliest and highest source of viral titer of the entire brain, suggesting early entry into the brain through this route. Interestingly, the cervical lymph nodes showed viral titers as early as one day post infection, and remained in higher titers until after three days post infection where the virus appeared to wane. The early replication of the virus without any clinical signs suggests that the virus must reach a critical mass of replication before it is able to cause symptoms, which tends to occur around five days post infection.

With the use of FITC salt, the blood brain barrier integrity was tested on a serial sacrifice experiment on Lewis rats. The low molecular weight FITC salt was injected via tail vein into the blood, and able to detect small breakages in the barrier by infiltrating into the brain. Using this method, there was no discernable breakdown of the barrier until day 5 post infection, where the FITC salt was able to flow easily into the tissues. Although the MMP-9 data suggested an early breakdown, the FITC salt was unable to penetrate the barrier at day 3 post infection. This may mean that MMP-9 is initially dysregulated, but quickly kept in check, before finally overcoming these restraints and breaking down the barrier. The use of Superhance 680 allowed for a more detailed exploration into this breakdown during the clinical disease window while the rats were still alive. At five days post infection, the brains were saturated with the agent compared to the controls. At six days post infection, there was still significantly more agent in the brain, which was further confirmed when the brains were imaged ex vivo to eliminate any interference from the rodent's head or body. Earlier imaging of infected rats days 1 to 4 post infection did not yield any significant results.

The FITC salt and Superhance 680 experiments supported the idea that RVFV enters the brain by a method other than the blood brain barrier, most likely directly through the olfactory bulb as the PCR data suggests. However, these studies have shown that MMP-9 is present in high levels in the brain of sick rats. The exact role that MMP-9, as well as other MMPs, plays in the integrity of the blood brain barrier and clinical disease remains a focus of investigation in the lab.

The predominant conclusion from these Lewis rat experiments is that the virus follows a route through the olfactory epithelium into the olfactory bulbs early during infection. Here, the virus is capable of replicating into high titers and avoids the immune system due to the presence of the blood brain barrier. Once the virus has established itself, it then breaks down the blood brain barrier while inflicting severe encephalitis on its host, ultimately leading to death. Further testing will need to be performed to verify without a doubt that the olfactory epithelium is the route of neuroinvasion, but these results have shown that it is the most likely route.

Rift Valley Fever is an understudied virus with a disease course that is not fully understood. The data presented here suggests that the olfactory epithelium may play a role regarding the early entry during cases of encephalitis caused by the virus. This is accompanied by a cytokine storm that occurs, dysregulating major processes as a result. With the use of novel *in vitro* models for both neuronal and blood brain barrier epithelial infection, the pathological effects of Rift Valley Fever Virus can be better understood during the course of a CNS infection.

5.1   PUBLIC HEALTH SIGNIFICANCE

The public health significance of this project is two-fold. First, this project highlights the creation of a novel *in vitro* model for both human neuronal and human blood brain barrier infection by Rift Valley Fever. Initial therapeutic cytotoxicity testing must be performed using *in vitro* experiments first before animal models are used to assess for adverse outcomes. The SH-SY5Y and HBMEC cells provide a great model for these exact reasons. They are very permissive to infection, and appear to create the same cytokine response as seen using the *in vivo* Lewis rat model.   In addition, the neuropathogenic model of Rift Valley Fever has been expanded upon as a result of these experiments. There is very little known at this time in regards to the neuropathogenesis of the virus during infection. However, the results shown here demonstrate that the virus is reaching the brain when infected by aerosol as early as one day post infection. This suggests that rather than entering through the breakdown of the blood brain barrier, the virus is entering into the olfactory epithelium directly. Future therapeutics will therefore need to focus on olfactory protection from infection. In addition, this virus has shown to cause a breakdown of the blood brain barrier, which coincides both with the clinical window of disease, as well as significant increases in MMP-9. This creates a possible target for therapeutics that may rely on preventing MMP-9 from activating, thus preventing a breakdown of the blood brain barrier, and ultimately stopping the clinical window from occurring. Further research is required to explore these possibilities, but

the ground work for these experiments has been laid by the results found in these studies. A clear understanding of a disease is required before an effective therapeutic or vaccine can be developed. The work presented here has added to the neuropathogenic model of disease caused by Rift Valley Fever Virus, providing more avenues for exploration to combat this pathogen.

BIBLIOGRAPHY

1.	Swanepoel, R. and J. Coetzer, *Rift valley fever.* Infectious diseases of livestock, 2004. **2**: p. 1037-1070.
2.	Balkhy, H.H. and Z.A. Memish, *Rift Valley fever: an uninvited zoonosis in the Arabian peninsula.* International journal of antimicrobial agents, 2003. **21**(2): p. 153-157.
3.	Bird, B.H., et al., *Rift Valley fever virus.* Journal of the American Veterinary Medical Association, 2009. **234**(7): p. 883-893.
4.	Hartman, A.L., et al., *Aerosolized Rift Valley Fever virus causes fatal encephalitis in African green monkeys and common marmosets.* Journal of virology, 2014. **88**(4): p. 2235-2245.
5.	Ludlow, M., et al., *Neurotropic virus infections as the cause of immediate and delayed neuropathology.* Acta neuropathologica, 2016. **131**(2): p. 159-184.
6.	Ikegami, T. and S. Makino, *The pathogenesis of Rift Valley fever.* Viruses, 2011. **3**(5): p. 493-519.
7.	Ikegami, T. and S. Makino, *Rift valley fever vaccines.* Vaccine, 2009. **27**: p. D69-D72.
8.	Carroll, M.C., *Lab 257.* 2009: Harper Collins.
9.	Rusnak, J.M., et al., *Immunogenicity and safety of an inactivated Rift Valley fever vaccine in a 19-year study.* Vaccine, 2011. **29**(17): p. 3222-3229.
10.	Caplen, H., C. Peters, and D.H. Bishop, *Mutagen-directed attenuation of Rift Valley fever virus as a method for vaccine development.* Journal of General Virology, 1985. **66**(10): p. 2271-2277.
11.	Peters, C., et al., *Prophylaxis of Rift Valley fever with antiviral drugs, immune serum, an interferon inducer, and a macrophage activator.* Antiviral research, 1986. **6**(5): p. 285-297.
12.	Caroline, A.L., et al., *Broad spectrum antiviral activity of favipiravir (T-705): protection from highly lethal inhalational rift valley fever.* PLoS Negl Trop Dis, 2014. **8**(4): p. e2790.
13.	Rich, K.M. and F. Wanyoike, *An assessment of the regional and national socio-economic impacts of the 2007 Rift Valley fever outbreak in Kenya.* The American journal of tropical medicine and hygiene, 2010. **83**(2 Suppl): p. 52-57.
14.	Turell, M.J., et al., *Potential for North American Mosquitoes to Transmit Rift Valley Fever Virus 1.* Journal of the American Mosquito Control Association, 2008. **24**(4): p. 502-507.
15.	Martin, V., et al., *The impact of climate change on the epidemiology and control of Rift Valley fever.* Revue Scientifique et Technique, Office International des Epizooties, 2008. **27**(2): p. 413-426.

16.   Rolin, A.I., L. Berrang-Ford, and M.A. Kulkarni, *The risk of Rift Valley fever virus introduction and establishment in the United States and European Union.* Emerging microbes & infections, 2013. **2**(12): p. e81.

17.   Mandell, R.B. and R. Flick, *Rift Valley fever virus: a real bioterror threat.* Journal of Bioterrorism & Biodefense, 2012. **2011**.

18.   Sidwell, R.W. and D.F. Smee, *Viruses of the Bunya-and Togaviridae families: potential as bioterrorism agents and means of control.* Antiviral research, 2003. **57**(1): p. 101-111.

19.   Peters, C.J. and M. Olshaker, *Virus hunter: thirty years of battling hot viruses around the world.* 1997: Anchor Books.

20.   Smith, D.R., et al., *The pathogenesis of Rift Valley fever virus in the mouse model.* Virology, 2010. **407**(2): p. 256-267.

21.   Peters, C. and T. Slone, *Inbred rat strains mimic the disparate human response to Rift Valley fever virus infection.* Journal of medical virology, 1982. **10**(1): p. 45-54.

22.   Bales, J.M., et al., *Choice of inbred rat strain impacts lethality and disease course after respiratory infection with Rift Valley Fever Virus.* Front Cell Infect Microbiol, 2012. **2**: p. 105.

23.   Bird, B.H., et al., *Rift valley fever virus lacking the NSs and NSm genes is highly attenuated, confers protective immunity from virulent virus challenge, and allows for differential identification of infected and vaccinated animals.* Journal of virology, 2008. **82**(6): p. 2681-2691.

24.   Ross, T.M., et al., *Animal models of Rift Valley fever virus infection.* Virus research, 2012. **163**(2): p. 417-423.

25.   Tung, W.H., et al., *Japanese encephalitis virus induces matrix metalloproteinase‐9 in rat brain astrocytes via NF‐κB signalling dependent on MAPKs and reactive oxygen species.* British journal of pharmacology, 2010. **161**(7): p. 1566-1583.

26.   Drummond, C.G., C.A. Nickerson, and C.B. Coyne, *A Three-Dimensional Cell Culture Model To Study Enterovirus Infection of Polarized Intestinal Epithelial Cells.* 2015.

27.   Caroline, A.L., et al., *Inflammatory biomarkers associated with lethal Rift Valley fever encephalitis in the Lewis rat model.* Frontiers in microbiology, 2015. **6**.